AMASYA UNIVERSITY
CENTRAL RESEARCH LABORATORY

International Journal of Science Letters (IJSL)

e-ISSN: 2687-4733
Year: 2024
Volume: 6
Number: 1

Management Office

Amasya University, Central Research Laboratory, 05100, Ipekkoy, Amasya

Legal Responsibility

From The Editor;

Dear Readers and Authors,

As “International Journal of Science Letters (IJSL)”, we are pleased and honored to present the first issue of 2024. IJSL, is an international double peer-reviewed open access academic journal published on the basis of research- development and code of practice.

The aims of this journal are to contribute in theoretical and practical applications in relevant researchers of Life Sciences, Biology, Biotechnology, Bioengineering, Agricultural Sciences, Food Biotechnology and Genetics institutions and organizations in Turkey, and to publish solution based papers depending on the principle of impartiality and scientific ethics principles, focusing on innovative and added value work, discussing the current and future.

With these thoughts, we are especially thankful to academicians honoring with the articles, valuable scientists involved in editorial boards and reviewers for their contributions to the evaluation processes with through their opinions/ideas/contributions/criticisms in this issue of International Journal of Science Letters.

16.03.2024

Editor in Chief

Prof. Dr. Tuba YILDIRIM

Contents

Yücel Tartan and Karavin, International Journal of Science Letters (IJSL). 2024. 6(1): 353-361
https://doi.org/10.38058/ijsl.1279005

Research Article

Effect of microplastics on dry matter content in *Lactuca sativa* L.

Gizem Yücel Tartan[1], Neslihan Karavin[2]*

[1]Amasya University, Institute of Science, Department of Biology
[2]Amasya University, Faculty of Art and Science, Department of Biology

*Correspondence: nnecli@gmail.com

Abstract

Plastics are commonly used in every field of life due to their ease of use and economics. If the plastic wastes are not disposed of properly, they form microplastics by breaking down into smaller particles with decomposition. Microplastics are chemical substances in polymer structure. They are difficult to dissolve in nature and require a long time. Microplastics, that spread to the environment in various ways, cause pollution and negatively affect organisms and ecosystems.

This study aimed to determine the effects of microplastics and the combined impact of microplastics and Cd on dry matter content (the ratio of dry mass to fresh mass of an organ), which is the one of the major plant traits for plant growth, in lettuce (*Lactuca sativa* L.). Five experiment sets were designed by using Simila variety lettuce seedlings, including (1) control, (2) 1.5 % microplastic (3) 2.5 % microplastic, (4) 1.5 % microplastic and 200 ppm Cd solution and (5) 2.5 % microplastic and 200 ppm Cd solution added. The polyethylene mulch pieces (2,5 mm x 4 mm) were used as microplastics. Results showed that the polyethylene microplastic addition to the soil significantly reduced aboveground and belowground DMCs of lettuce seedlings. Concentration of the microplastics in the soil was also effective on DMC. The Cd addition to the soils, which contain microplastics, a bit increased the DMC.

Article History

Received 07.04.2023
Accepted 27.04.2023

Keywords

Dry matter content,
Lettuce,
Microplastic,
Mulch,
Pollution.

1. Introduction

The plastics are one of the major problems that threaten the health and wellness of living things and sustainability of environment. Plastics, that do not occur naturally on earth, are obtained by reacting monomers with a catalyst under a certain temperature and pressure. Plastics are used in every field of life and cause pollution through domestic, industrial, and medical wastes. According to the previous researches, it has been revealed that plastic pieces

are found in many places from the poles to deserted islands and the deepest point of the world (Yurtsever, 2019). The plastics are polymers made from petroleum materials and difficult to dissolve in nature. They turn into microplastics in various types and shapes when decomposed. The microplastic term is firstly used by Thompson in 2004. Microplastics are generally called as plastic particles smaller than 5 mm in size (Bouwmeester et al., 2015). They were defined in more detail as "regular or irregularly shaped synthetic solid particles or polymeric matrices originating from primary or secondary production, insoluble in water, varying in size from 1 mm to 5 mm" (Frias and Nash, 2019, Arı and Öğüt, 2021). Microplastics have many characteristic physicochemical properties such as having a hydrophobic surface, transporting and absorbing pollutants, and thermooxidation. Most of the sources of microplastics are the synthetic textile fibers, microbeads found in fertilizers, drugs, detergents and toothpastes, bags, scraps, pieces, debris, particles from automobile tires, greenhouse nylons, plastic mulching materials, irrigation pipes.

Because the microplastics are small enough to be easily transported from one ecosystem to another, they have became a global problem as one of the major pollutants (Thompson et al., 2009). Microplastics are transported to ecosystems by various ways and cause pollution. Microplastic pollution leads to various damages due to their presence in the environment and accumulation in the bodies of living things. They not only threaten the extinction of living things by disrupting terrestrial and aquatic ecosystems, but also damage the natural order by changing the physical, chemical and biological properties of soil and water (Yurtsever, 2019). The microplastics, which are in very small sizes, enter the body of organisms through respiration, food and water, cause various disruptions in their metabolism. Because they can adsorb chemicals and heavy metals, microplastics are complex pollutants for living things (Rochman et al., 2013). Microplastics also affect the seed germination, uptake of nutrients and plant growth by changing the soil structure in terrestrial ecosystems. Studies on microplastics have been carried out mostly in aquatic ecosystems because of their easy detection. The effects of microplastics on the living organisms and soil in terrestrial ecosystems have not yet been fully understood due to the insufficient number of studies.

In the study of Wu et al. (2020), polystyrene microplastic (PSMP) stress was applied to *Oryza sativa* L. and after 21 days shoot biomass decreased based on low, medium and high dose applications as %13,1, %18,8 and %40,3, respectively. The amounts of 12 amino acids, 16 saccharides, 26 organic acids and 17 other components (lipids and polyols) in the leaves of 24 samples exposed to PSMP at doses of 50 mg L^{-1} and 250 mg L^{-1} with hydropoic culture

decreased. Li et al. (2020) applied PVC microplastic particles with sizes between 100 nm and 18 μm at 0.5%, 1% and 2% concentrations to the root systems and leaves of lettuce. Microplastics did not cause changes in root activity; but the total length, surface area, volume and diameter of the roots increased. They reported that superoxide dismutase activity increased by 1% in lettuce leaves and electron transfer, light absorption, diffusion and capture decreased. Khalid et al. (2020) determined that microplastics directly affect plants by clogging the seed pores, limiting the uptake of water and soil compounds, as well as causing accumulation in leaves, roots and stems. Indirectly, they change the physicochemical structure of the soil by affecting the microbes and fauna in the soil.

Dry matter content, which is the ratio of dry mass to fresh mass of an organ, is a useful plant trait for understanding the plant status, production and life strategies. Since dry matter content provides information about plant production, research use and water content, it is commonly used as an ecophysiological parameter in plant studies (Garnier et al. 2001, Grime et al. 1997)

In this study, it was aimed to determine the effects of microplastics and the combined impact of microplastics and Cd on dry matter content in lettuce (*Lactuca sativa* L.). We hypothesized that the microplastic addition to the soil would be decrease DMCs and the combined effect of microplastics and Cd, which are the two of the major pollutants in most of the agricultural areas, may leads to lower DMC.

2. Materials and Methods

2.1 Experimental Design

In this study, Simila variety lettuce seedlings were used as plant material. Lettuce seedlings were produced from certified seeds by Alp Fide in Amasya, Turkey. To determine the effect of microplastics and the combined impact of microplastics and Cd on dry matter content in lettuce, fivefactorial experiment set was designed, including (1) control, (2) 1.5 % microplastic (3) 2.5 % microplastic, (4) 1.5 % microplastic and 200 ppm Cd solution and (5) 2.5 % microplastic and 200 ppm Cd solution added. Each experiment set was performed with six repetitions.

Figure 1. Experiment sets of lettuce

A total of 60 lettuce seedlings were studied. Because of its common usage in agriculture as a cover material for production, microplastics were obtained by cutting the polyethylene mulch into 2,5 mm x 4 mm pieces. The garden soil taken at a depth of 0-25 cm was mixed with the peat in 50 % volume. The microplastics were added to the soils in relevant experimental sets. All the pots were irrigated in an equal amount water on alternate day.

2.2 Dry Matter Content

After 28 days, the lettuce seedlings were harvested by carefully separating from the soil. The fresh weights of the aboveground and the underground parts of the lettuce seedlings were immediately measured with scales. Then, they were oven-dried in paper bags at 65 ^{o}C until the constant weight reached and the dry weights of the lettuce seedlings were measured.

Figure 2. Harvested lettuce seedlings

The dry matter contents of aboveground and underground parts of the lettuce seedlings were calculated as dry mass per unit fresh mass (mg g^{-1}). The statistical analyses were performed by SPSS 20.0 statistical software. The differences in means among the treatments were determined by one-way ANOVA.

3. Results and Discussion

Results showed that both the aboveground and the belowground DMCs of the lettuce seedlings significantly varied based on microplastic and microplastic+Cd additions. The maximum aboveground and belowground DMCs were found in the control groups. The minimum aboveground and belowground DMCs were found in the lettuce seedlings grown in 1.5% microplastic added pots. DMC significantly decreased based on microplastic addition. Amount of the microplastics also changed the DMC in both aboveground parts and belowground of the lettuce seedlings. However, Cd addition to the soils, which also contain microplastics, altered the DMC. The combined applications of the microplastics and the Cd solution led to a bit increase in DMC in the aboveground parts and the belowground of the lettuce seedlings. The belowground DMCs (> 50 mg g^{-1}) of the lettuce seedlings were higher than the aboveground DMCs (<50 mg g^{-1}).

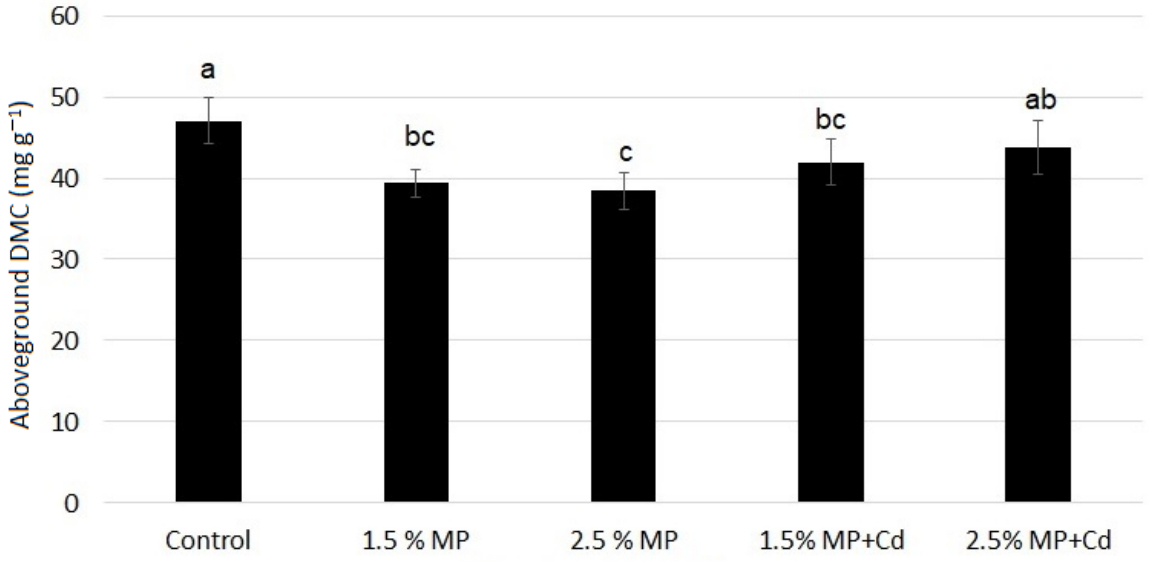

Figure 3. Variation in the aboveground DMCs (mg g^{-1}) of the lettuce seedlings (MP: Microplastic)

Table 1. Significance of variation in the aboveground DMC (mg g^{-1}) among the experiment sets

Aboveground DMC (mg g^{-1})	Sum of Squares	df	Mean Square	F	P
	289.574	4	72.393	10.676	0.000

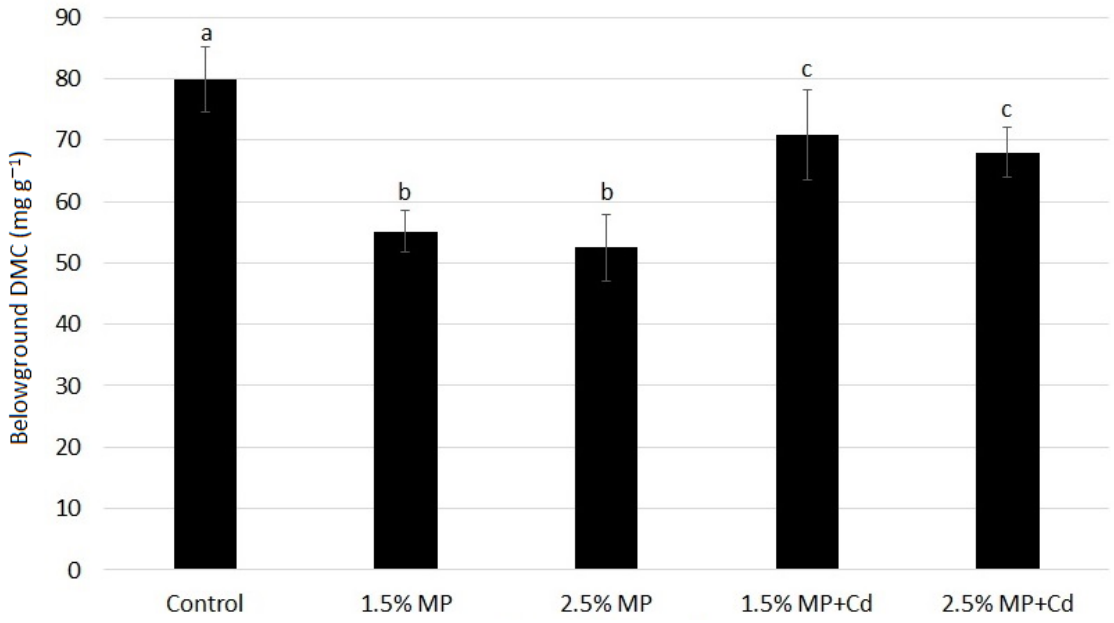

Figure 4. Variation in the belowground DMCs (mg g^{-1}) of the lettuce seedlings (MP: Microplastic)

Table 2. Significance of variation in the belowground DMC (mg g^{-1}) among the experiment sets

Belowground DMC (mg g^{-1})	Sum of Squares	df	Mean Square	F	P
	3119.155	4	779.789	28.246	0.000

Similar results were obtained in the some of the previous studies. In the study of Wang et al. (2021), while 0,1% MPs+Cd and 1% MPs+Cd additions did not cause any variation, the co-addition of Cd and 10% MPs decreased the plant biomass in lettuce. More than 25.9% biomass reduction was determined in crops exposed to polystyrene microplastic particles (PSMP) 142 days after planting by Wu et al. (2020). In the study of Enyoh et al. (2020), the root biomass of *Citrus aurantium* L. was negatively affected by the plastic addition. Additionally, they found that the microplastics exhibited greater negative effects than macroplastics. Qi et al. (2018) reported that wheat (*Triticum aestivum* L.) plant performance parameters such as leaf area decreased with the addition of biodegradable plastic mulch residue. Furthermore, significantly lower shoot biomass was determined in wheat plants grown in starch-based biodegradable microplastic added soils while no significant variation

was found in those grown in low-density polyethylene microplastics. Total plant biomass of wheat was significantly decreased due to the addition of plastics to the soil. They emphasized that aboveground and the belowground parts of the wheat plants negatively affected by the microplastic addition. Our results coincided with the previous studies that reported the negative effects of the microplastics to the plant growth.

As a conclusion, polyethylene microplastic addition to the soil significantly reduced the aboveground and the belowground DMCs of the lettuce seedlings. The concentration of the microplastics in the soil was also effective on DMC. The Cd addition to the soils which also contain the microplastics a bit increased the DMC.

In recent years, plastic pollution became a basic problem in the world. One of the major sources of the plastic pollution is the intensive usage of plastic mulching in agriculture. Since they are difficult to dissolve in nature and easily transportable, microplastics are important pollutants in both aquatic and terrestrial ecosystems. They change the features of soil and water and cause damages in organisms. Because of their importance for health of organisms and ecosystems, future detailed studies are required to understand the effects of microplastics on plant traits and growth performance.

References

Arı, M. and Öğüt, S. 2021. Mikroplastikler ve çevresel etkileri. Düzce Üniversitesi Bilim ve Teknoloji Dergisi, 9(2), 864-877.

Bouwmeester, H., Hollman, P.C., Peters, R.J. 2015. Potential health impact of environmentally released micro-and nanoplastics in the human food production chain: experiences from nanotoxicology. Environmental Science & Technology, 49(15), 8932-8947.

Enyoh, C.E., Verla, A.W., Verla, E.N., & Enyoh, E.C. 2020. Effect of macro-and micro-plastics in soil on quantitative phytochemicals in different part of juvenile lime tree (*Citrus aurantium*). International Journal of Environmental Research, 14(6), 705-726.

Frias, J.P. and Nash, R. 2019. Microplastics: Finding a consensus on the definition. Marine Pollution Bulletin, 138, 145-147.

Garnier, E., Shipley, B., Roumet, C., Laurent, G. 2001. A standardized protocol for the determination of specific leaf area and leaf dry matter content. Functional ecology, 15(5), 688-695.

Grime, J.P., Thompson, K., Hunt, R., Hodgson, J.G., Cornelissen, J.H.C., Rorison, I.H., ... Whitehouse, J. (1997). Integrated screening validates primary axes of specialisation in plants, Oikos, 79(2), 259-281.

Khalid, N., Aqeel, M., Noman, A. 2020. Microplastics could be a threat to plants in terrestrial systems directly or indirectly. Environmental Pollution, 267, 115653.

Li, Z., Li, Q., Li, R., Zhao, Y., Geng, J., Wang, G. (2020). Physiological responses of lettuce (*Lactuca sativa* L.) to microplastic pollution. Environmental Science and Pollution Research International, 27, 30306-30314.

Qi, Y.L., Yang, X.M., Pelaez, A.M., Lwanga, E.H., Beriot, N., Gertsen, H., Garbeva, P., Geissen, V. 2018. Macro- and micro- plastics in soil-plant system: effects of plastic mulch film residues on wheat (*Triticum aestivum*) growth. Science of the Total Environment, 645, 1048-1056.

Rochman, C.M., Hoh, E., Kurobe, T., Teh, S.J. 2013. Ingested plastic transfers hazardous chemicals to fish and induces hepatic stress. Scientific Reports, 3(1), 1-7.

Thompson, R.C., Moore, C.J., vom Saal, F.S., Swan, S.H. 2009. Plastics, the environment and human health: current consensus and future trends. Philos Trans. R. Soc. Lond B. Biology Science, 364(1526), 2153-66.

Wang, F., Wang, X., Song, N. 2021. Polyethylene microplastics increase cadmium uptake in lettuce (Lactuca sativa L.) by altering the soil microenvironment. Science of the Total Environment, 784, 147133.

Wu, X., Liu, Y., Yin, S., Xiao, K., Xiong, Q., Bian, S., ... Yang, J. 2020. Metabolomics revealing the response of rice (*Oryza sativa* L.) exposed to polystyrene microplastics. Environmental Pollution, 266, 115159.

Yurtsever, M. and Yurtsever U. 2019. Use of a convolutional neural network for the classification of microbeads in urban wastewater. Chemosphere, 216, 271-280.

Türkmen Bulca and Yakalı, International Journal of Science Letters (IJSL). 2024. 6(1): 362-376
https://doi.org/10.38058/ijsl.1300611

Research Article

Estimation of the Charge Mobility of Phenanthroline derivatives with the view of Density Functional Theory: Reorganization Energy and Charge Transfer Integral are in play

Zeynep Türkmen Bulca[1], Gül Yakalı[2*]

[1] Nanoscience and Nanotechnology Program, Institute of Science, Izmir Katip Çelebi University, Izmir, Turkey
[2] Department of Engineering Sciences, Faculty of Engineering, Izmir Katip Çelebi University, Izmir, Turkey

*Correspondence: gul.yakali@ikcu.edu.tr

Abstract

Molecular arrangement and noncovalent interactions in organic materials greatly influence the charge mobility in organic light-emitting diodes (OLEDs), organic photovoltaics (OPVs), and organic field-effect transistors (OFETs). In the light of the this argument, we examined the electronic properties of the phenanthroline derivatives by considering the charge mobility with the combination of density functional theory and Marcus Charge Transfer Theory. The drift electron mobility of the molecule **1** and **2** were determined to 21.13 $cm^2\ V^{-1}\ s^{-1}$ and 18.00 $cm^2\ V^{-1}\ s^{-1}$, respectively through J type $\pi \cdots \pi$ stacking interactions created by small perpendicular distances between the adjacent rings. The effective charge pathways of the molecules were generated with strong $\pi \cdots \pi$ stacking interactions consolidated by noncovalent interactions in their solid phases. The electron reorganization energy for both molecules were determined smaller than that of holes which means they have n-type semiconductor properties. The charge transfer integrals were calculated with the optimization of molecules' dimer configurations that the theoretical results demonstrate the charge transfer integral depends on the distance between the stacking rings. High charge transfer integral and small reorganization energy give the high charge mobility fort he semiconductor molecules. Beside the mobility, energy band gap, ionization potential, electron and hole injection barriers of the molecules were interpreted to further understand their electronic properties. Due to the small LUMO values which provide n-type molecule and small electron injection barrier. From the our work both molecules can be effective n type organic semiconductor devices with the high mobility and can be modified for more efficient charge transport in phenanthroline derivatives.

Article History

Received 22.05.2023
Accepted 17.02.2024

Keywords

n-type organic semiconductor devices, DFT, J type $\pi \cdots \pi$ stacking, charge mobility, phenanthroline derivatives.

1. Introduction

Molecular arrangement and noncovalent interactions in organic materials greatly influence the charge mobility in organic light-emitting diodes (OLEDs), organic photovoltaics (OPVs), and organic field-effect transistors (OFETs). In the light of the this argument, we examined the electronic properties of the phenanthroline derivatives by considering the charge mobility with the combination of density functional theory and Marcus Charge Transfer Theory. The drift electron mobility of the molecule **1** and **2** were determined to 21.13 $cm^2\ V^{-1}\ s^{-1}$ and 18.00 $cm^2\ V^{-1}\ s^{-1}$, respectively through J type $\pi \cdots \pi$ stacking interactions created by small perpendicular distances between the adjacent rings. The effective charge pathways of the molecules were generated with strong $\pi \cdots \pi$ stacking interactions consolidated by noncovalent interactions in their solid phases. The electron reorganization energy for both molecules were determined smaller than that of holes which means they have n-type semiconductor properties. The charge transfer integrals were calculated with the optimization of molecules' dimer configurations that the theoretical results demonstrate the charge transfer integral depends on the distance between the stacking rings. High charge transfer integral and small reorganization energy give the high charge mobility fort he semiconductor molecules. Beside the mobility, energy band gap, ionization potential, electron and hole injection barriers of the molecules were interpreted to further understand their electronic properties. Due to the small LUMO values which provide n-type molecule and small electron injection barrier. From the our work both molecules can be effective n type organic semiconductor devices with the high mobility and can be modified for more efficient charge transport in phenanthroline derivatives.

2. Theoretical Methodology

Density functional theory studies are a widely used computational method to understand the optical and electronic properties of organic materials. B3LYP-6311G (d, p) basis set was used with the Gaussion 09 software in this study (Reed *et al.*, 2014). The optimizede geometries of the neutral and charged states of the molecules were determined form cif file obtained by single crystal x-ray diffraction experiment. The charge trasnfer integral and reorganization energy, iyonization potential and electron affinity, charge transfer rate and mobility of the molecules were calculated by the combination of DFT and Marcus electron theory formula given in the equation 1.

$$k = \frac{4\pi^2}{\lambda}\frac{1}{\sqrt{4\pi h k_B T}} t^2 \exp\left(-\frac{\lambda}{4k_B T}\right) \quad (1)$$

The reorganization energy (λ) includes; inner reorganization energy includes the geometric changes in the molecules and is the modifications in the molecular geometry if an electron, is removed or added to a molecule. The inner reorganization energy is divided into two parts: λ^1 represents the geometry relaxation energy of one molecule from neutral to charged state, λ^2 represents the geometry relaxation energy from charged to neutral state (Yang *et al.*, 2019).

$$\lambda = \lambda_{rel}^1 + \lambda_{rel}^2 \quad (2)$$

In the evaluation of λ, the two terms were computed directly from the adiabatic potential energy surfaces.

$$\lambda_{anion} = \lambda_{rel}^1 + \lambda_{rel}^2 = \left[E^{(0)}(M^-) - E^{(0)}(M)\right] + \left[E^{(1)}(M) - E^{(1)}(M^-)\right] \quad (3)$$

$$\lambda_{cation} = \lambda_{rel}^1 + \lambda_{rel}^2 = \left[E^{(0)}(M^+) - E^{(0)}(M)\right] + \left[E^{(1)}(M) - E^{(1)}(M^+)\right]$$

where $E^0(M^+)$ and $E^0(M)$ represent the energies of the neutral molecule at the cation geometry and at the optimal ground-state geometry respectively. $E^1(M)$ and $E^1(M+)$ represent the energy of the charged state at the neutral geometry and optimal cation geometry, respectively. In the calculation of ionization energy, the adiabatic ionization potential (IPa) and vertical ionization potential (IPv), the adiabatic/vertical electron affinity (EAa)/(EAv) of both molecules have been calculated as the following equation.

$$IPa = E^0(M)^+ - E^0(M) \text{ and } IPv = E^1(M)^+ - E^0(M) \quad (4)$$

$$EAa = E^0(M) - E^0(M)^- \text{ and } EAv = E^0(M) - E^1(M)^-$$

The charge transfer integral of the molecules was calculated by using the DFT optimized molecular configuration for its dimeric structure given in the Figure 2. Using the DFT optimized molecular configurations for dimeric structures of the molecule 1 and 2 created by the pi···pi stacking interactions, the charge transfer integral of the both molecules were determined. In the formation of the dimeric structure with two isolated molecules, two HOMO (LUMO) levels from each molecule combines to make HOMO and HOMO-1 (LUMO and LUMO+1) in a dimer. In a simplified energy splitting in dimer, the charge transfer integral (t) is approximated as the half of the energy difference between HOMO and HOMO-1 for hole transfer whereas LUMO and LUMO+1 for electron transfer. (Köse *et al.*, 2007)

$$t_{hole} = \frac{HOMO - HOMO-1}{2} \qquad t_{electron} = \frac{LUMO - LUMO+1}{2} \quad (5)$$

To estimate the transfer integral of the molecules, we have take into account perpendicular distances between the adjacent rings is 3.947Å for the molecule 1 and 3.77 Å and 3.44 Å fort he molecule 2. Two dimeric configurations were considered to calculate the charge transfer integral of the molecule 2. The formula of the diffusion coefficient associated to a one-dimensional jumping process is given in the equation 6.

$$D = K_B d^2 \quad (6)$$

The mobility, μ, can be obtained from the following expression where e is the electron charge d is the transport distance from the molecular center to center in a stacking dimer, k_B is the Boltzmann constant and T was taken 300 K (Huang *et al.*, 2020).

$$\mu = \frac{eD}{kT} = \frac{ed^2 k_T}{k_B T} \quad (7)$$

3. Results and Discussion

3.1. Prediction of charge transport properties of the molecules

The crystal structure of the **molecule 1** (2,7-dibütylbenzo[lmn][3,8] phenanthroline-1,3,6,8(2H,7H)-tetrone) and **molecule 2** (2,7-dipropylbenzo[lmn][3,8]phenanthroline-1,3,6,8(2H,7H)-tetrone) were taken from Cambridge crystallographic database sample 819749 (a = 5.2230(10)Å, b =7.840(2) Å , c = 11.132(3) Å, Z = 4 and $\alpha = 103.716(2)°, \beta = 94.279(2)°, \gamma = 93.858(3)°$) and sample 1029340 (a = 6.9622(4)Å, b =17.2426(11) Å , c = 27.5809(15) Å, Z = 4 and $\alpha = 90°, \beta = 90°, \gamma = 90°$) (Huang *et al.*, 2020; Krishna *et al.*, 2016). We investigated the charge transfer and electronic characteristic of the both molecules in terms of their hole and electron reorganization energies, charge transfer integral, energy gap, ionization potential (IP) and electron affinity (EA) and charge mobility as shown in Table 1. The optimized structures in the neutral state of the both molecules are presented in the Figure 1.

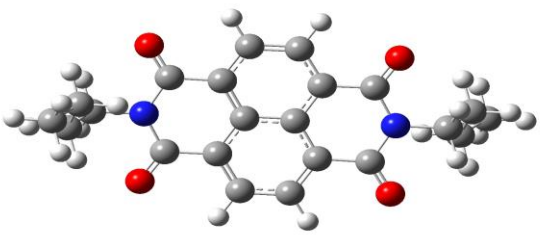

Molecule 1

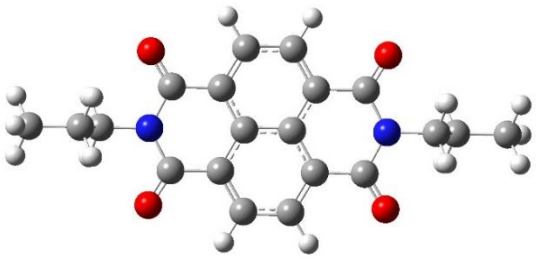

Molecule 2

Figure 1. Optimized geometry of the molecules in the neutral state.

Table 1. The value of parameters determining the charge transfer property of the molecules.

Molecule	λ_{hole} (eV)	$\lambda_{electron}$ (eV)	t_{elec}	t_{hole}	IPa (eV)	IPv(eV)	Ea(eV)	Ev(eV)	k_{hole} (s^{-1})	$k_{electron}$(s^{-1})
1	2.39	0.0030	0.086	0.025	8.61	10.9	2.30	2.12	1.1×10^{12}	3.5×10^{14}
2	0.0037	0.0036	0.038 (dimer 1) 0.78 (dimer 2)	0.016 (dimer 1) 0.14 (dimer2)	8.43	8.53	2.04	1.86	2.4×10^{13} 5.06×10^{15}	3.34×10^{14} 1.54×10^{17}

Molecules	d_L (Å)	μ_{hole} ($cm^2V^{-1}s^{-1}$)	$\mu_{electron}$ ($cm^2V^{-1}s^{-1}$)
1	3.947(3)	0.066	21.13
2	3.77(2)	1.3	18
2	3.44(2)	11	70

Reorganization energies of the molecule 1 for hole and electron transfer were calculated from adiabatic potentials are 2.39 and 0.003 eV, respectively. The reoragnization energies of te molecule 2 are 0.0037 eV for hole and 0.0036 eV for electron. Because of lower electron reorganization energy, it is suggested that bot molecules exhibit the higher intrinsic electron transfer rate, and hence, higher electron mobility than that of hole. Therefore, both molecules can be called n-type semiconductors. In terms of the dihedral angle in the crystal structure of the molecule 1 and 2 between the fragments we interpreted the reorganization energy. The dihedral angle for neutral state of molecule 1 is 76.95803 while this value were found as 79.33375 and 79.96829 for the cationic and anionic states, respectively. The cationic state

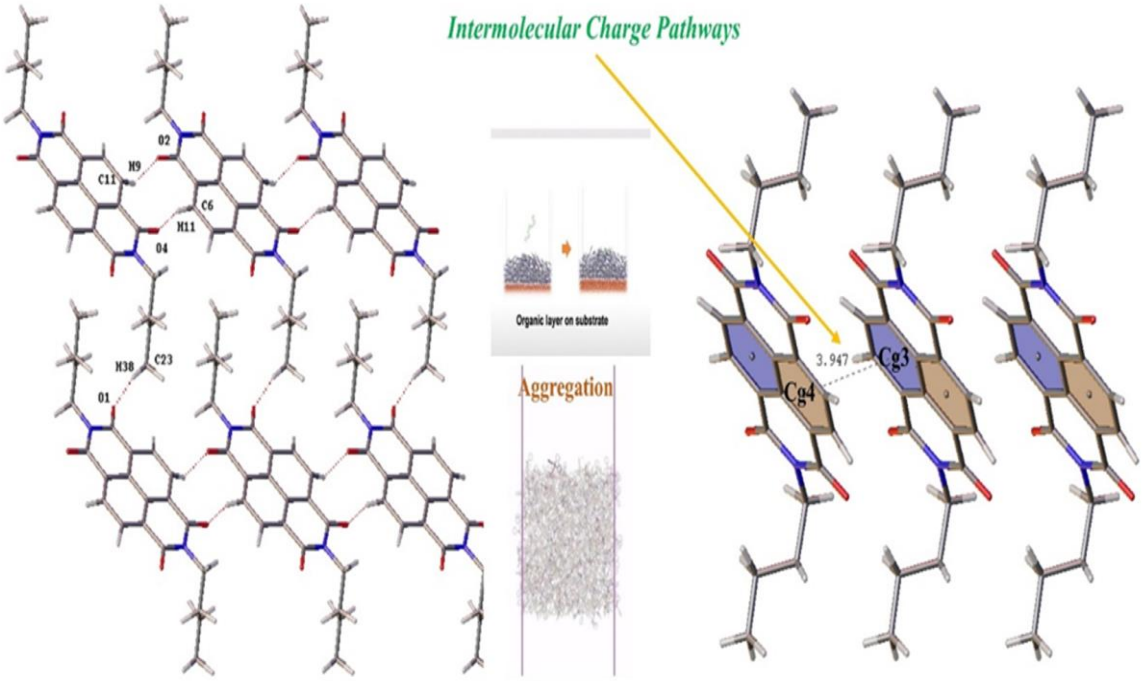

(010) plane **(110) plane**

is more dominant than anionic state in terms of the dihedral angle between the two rings. It means that electron reorganization energy is smaller than those of the hole. The charge carriers could be electrons. This situation were observed in the molecule 2 that the diheral angles for the neutral, anion and cation state were found as 179. 911°, 179.908° and 179.986°, respectively.

Molecule 1

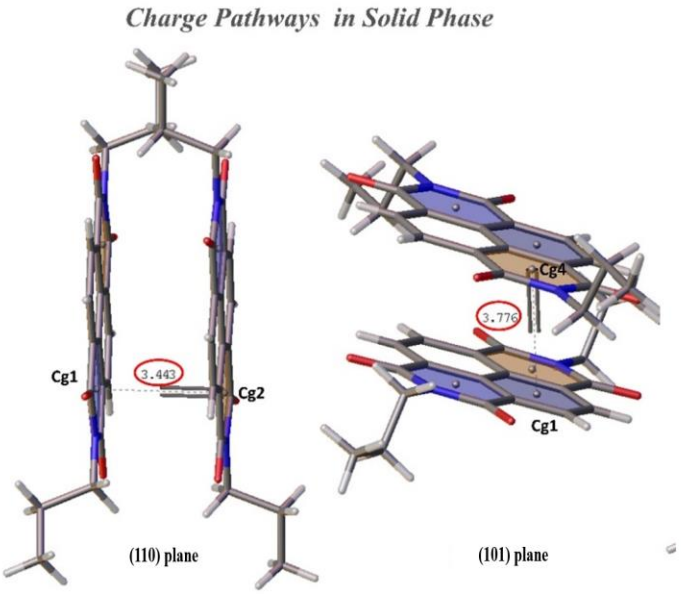

Molecule 2

Figure 2. Hopping pathways within crystal structure of the molecule 1 and molecule 2.

Charge transport properties strongly depend on the solid-state packing arrangements and orientations of the molecules including noncovalent interactions such as van der Waals interactions, π-π stacking, and hydrogen bondings (Alvey *et al.*, 2010; Cheng *et al.*, 2016). The reported crystalline structures of the molecules based on the X-ray diffraction analysis show the packing of molecules with the typical J type stacking consolidated with C-O…pi and nonclassical C-H…O hydrogen bods in their solid phases. Charge transfer integrals were obtained by from the geometries of the dimers optimized (B3LYP/6-31G(d, p)) where the center of mass distance and the angle between molecular planes were fixed by freezing the coordinate of the central rings. Since the dimers are symmetric and two monomers are equivalent under the symmetric transformation in the charge transfer process we can neglect the electrostatic polarization effect (Swicka *et al.*, 2018; Tan *et al.*, 2021).

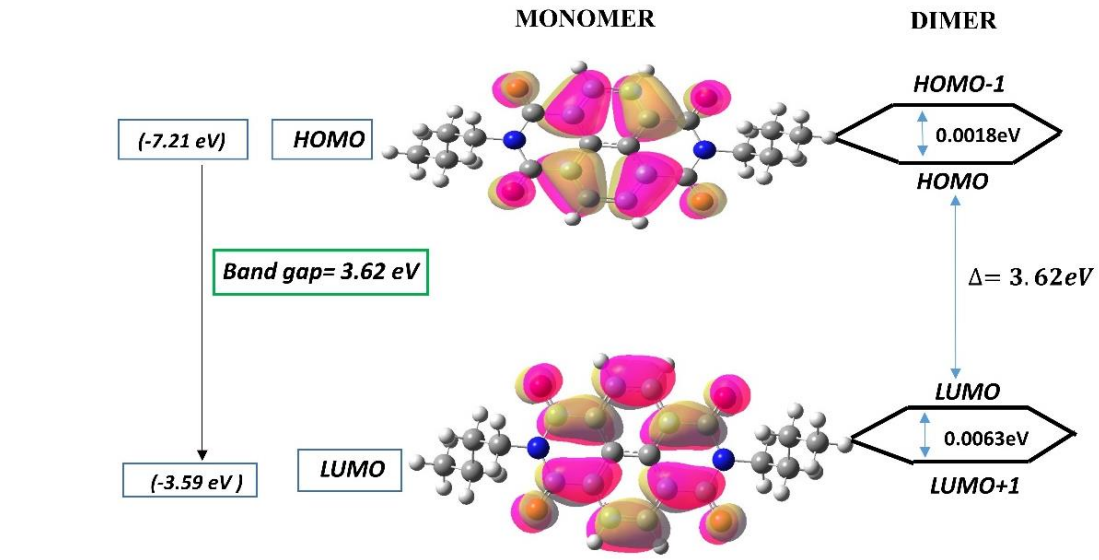

Molecule 1

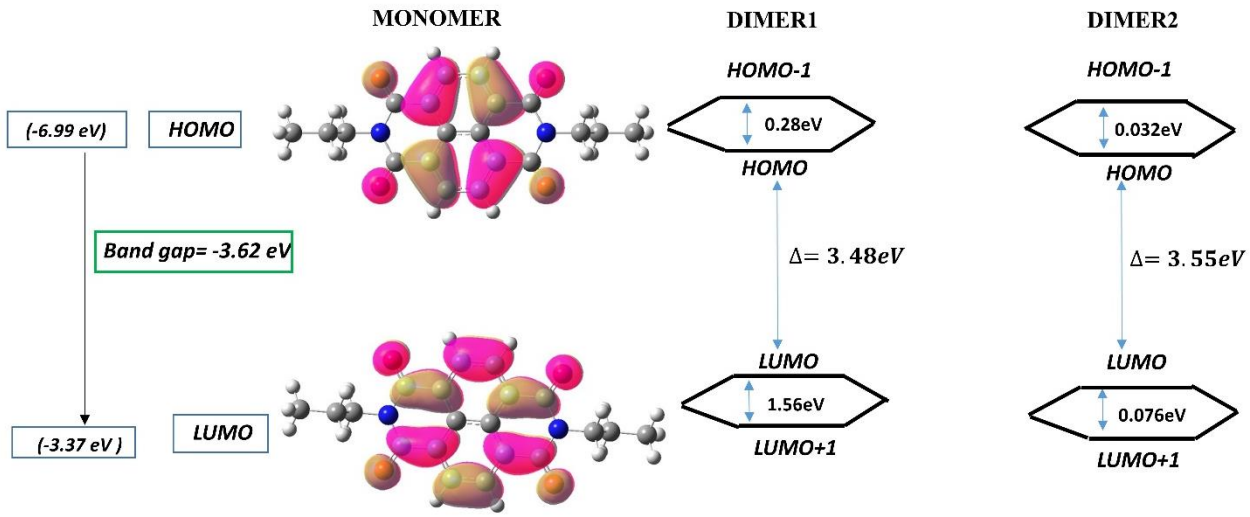

Molecule 2

Figure 3. Energy level diagram of the frontier orbitals for dimers of the both molecules in solid phase.

Fig. 3 describes the energy level diagram of dimer of the molecule 1 along 110 plane shown in Fig. 2. LUMO and HOMO levels of two monomers were combined and created LUMO+1, LUMO, HOMO and HOMO-1 in the dimer configuration. Along 110 plane, the energy level splitting between HOMO and HOMO-1 is about 0.0018 eV. In contrast, the energy splitting between LUMO and LUMO+1 is 0.0063 eV, which is 3.5 times higher, indicating a poor hole transport in this material. For the dimer 1of the molecule 2, the energy level splitting between HOMO and HOMO-1 is about 0.28 eV while that of LUMO and LUMO+1 is 1.5 eV which

supports molecule 2 is an efficient electron transfer molecule. This situaton is valid for the dimer 2 of the molecule 2. The charge trasnfer integral value of the dimeric 2 configuration of the molecule 2 has the highest value of 70 cm^2 V^{-1} s^{-1} due to the more stronger stacking interactions with the small perpendicular distance between the rings (3.44 Å). This charge pathway creates efficient charge transport in the molecule 2 along the (110) plane. Electron mobility by considering the expression for the diffusion coefficient associated to a one-dimensional jumping process was found greater than hole mobility for each dimeric configuration of the molecules which supports they show n-type semicondcutor material feature (Table 1).

The injection of the holes and electrons play an important role to create optimized electronic devices in real world (Yang *et al.,* 2008; Senevirathna *et al.,* 2014). The information about the organic device performance and its stability can be obtained from the parameters of ionization potential (IP) and electronic affinity (EA) that determine the charge injection through estimating the energy barrier for injection of hole and electron into molecule. The ionization energy describes the energy necessary to remove electrons from the neutral molecule to create cation molecule. The higher IP values indicate that the molecule is difficult to become cation in environment to react with OH- (H_2O) or O_2- (O_2) existing in the atmosphere. Hence, it is indicated that molecule 2 is more sensitive to the reaction with ion OH- or O_2. (Liu *et al.,* 2013; Huong *et al.,* 2013). While molecule 1 is more stable and hardly oxidized which can be favoured for the practical applications (Gruhn *et al*., 2002).

The EA values of molecule 1 and molecule 2 are 2.30 and 2.04 eV, respectively (Table 1). For the devices if the EA value is high, it means that injection energy for electron will be small (commonly used metallic electrodes (3 eV)). From these EA values, we can see that molecule 1 is better than molecule 2 for transporting electrons from both lowering the energy barrier for electron injection. Besides that, the HOMO energy levels for both compounds are not good aggrement with the work function of the gold electrode (-5.2 eV). Therefore, the injection of the hole from the gold to the organic semiconductor does not easily accompolished. For example, OFET is composed of a gate electrode, dielectric layer, organic semiconductor layer, and source-drain (S-D) electrodes. Carrier injection from the S-D electrode into the organic layer mainly depends on the barrier between the work function of the metal electrode and the HOMO or LUMO energy level of the organic semiconductors (Daswani *et al*., 2018).

N-type materials, typically have LUMO levels between –3 and –4 eV and have better contact with low work-function metals, such as calcium and lithium. The LUMO levels are 3.37 eV and 3.59 eV for both molecules.

4. Conclusions

Molecular packing in organic materials greatly influences the charge mobility in organic light-emitting diodes (OLEDs), organic photovoltaics (OPVs), and organic field-effect transistors (OFETs). Here, we have performed the calculation of the charge mobility in molecular crystals of phenanthroline derivatives by considering the reorganization energy fort he monomer molecules and carge transfer integral for the dimeric configurations of the molecules. With the combination of density functional theory and Marcus Charge Transfer Theory. The drift electron mobility of the molecule **1** and **2** were determined to 21.13 $cm^2\ V^{-1}\ s^{-1}$ and 18.00 $cm^2\ V^{-1}\ s^{-1}$, respectively through J type $\pi \cdots \pi$ stacking interactions created by small perpendicular distances between the adjacent rings. The electron reorganization energy for both molecules were determined smaller than that of holes which means they have n-type semiconductor properties. Due to the small LUMO values which provide n-type molecule and small electron injection barrier fort he molecules. Molecule 2 is more sensitive to the reaction with ion OH- or O_2 while molecule 1 is more stable and hardly oxidized which can be favoured for the practical applications due to the high ionization potential of the molecule 1. Electron mobility by considering the expression for the diffusion coefficient associated to a one-dimensional jumping process was found greater than hole mobility for each dimeric configuration of both molecules which supports they show n-type semicondcutor material feature. From the our work both molecules can be effective n type organic semiconductor devices with the high mobility and can be modified for more efficient charge transport in phenanthroline derivatives for applications in real word.

Acknowledgement

The author acknowledges Assoc. Prof. Dr. Muhittin Aygün studying at Dokuz Eylül University for technical contribution

Author contributions

Gül Yakalı wrote the whole manuscript and with Zeynep Türkmen Bulca performed and interpreted theoretical calculations.

Declarations

Conflict of interest

The authors declare that they have no conflict of interest.

Funding

The authors received no specific funding for this work.

References

Alvey P. M., Reczek J. J., Lynch V., and Iverson B. L. 2010. A Systematic Study of Thermochromic Aromatic Donor-Acceptor Materials. J. Org. Chem., 75, 7682–7690.

Chai S., Wen S., Huang J., and Han K. 2011. Density Functional Theory Study on Electron and Hole Transport Properties of Organic Pentacene Derivatives with Electron-Withdrawing Substituent. Journal of Computational Chemistry, 3218-3225.

Chakravarty M. and Vora A., 2021. Drug Delivery and Translational Research, 11, 748.

Chang Y. and Chao I. 2010. An Important Key to Design Molecules with Small Internal Reorganization Energy: Strong Nonbonding Character in Frontier Orbitals. J. Phys. Chem. Lett., 1, 116–121.

Cheng Y., Qi Y., Tang Y., Zheng C., Wan Y., Huang W., and Chen R. 2016. Controlling Intramolecular Conformation Through Nonbonding Interaction for Soft-Conjugated Materials: Molecular Design and Optoelectronic Properties. J. Phys. Chem. Lett., Just Accepted Manuscript.

Cias P., Slugovc C., and Gescheidt G. 2011. Hole Transport in Triphenylamine Based OLED Devices: From Theoretical Modeling to Properties Prediction. J. Phys. Chem. A, 115, 14519–14525.

Daswani U., Singh U., Sharma P., and Kumar A. 2018. From Molecules to Devices: A DFT/TD-DFT Study of Dipole Moment and Internal Reorganization Energies in Optoelectronically Active Aryl Azo Chromophores. J. Phys. Chem. C, Just Accepted Manuscript.

Gao H. 2010. Theoretical investigation into charge mobility in 4,40-bis(1-naphthylphenylamino) biphenyl. Theor. Chem. Acc. 127:759–763.

García-Frutos E. M., Gutierrez-Puebla E., Monge M. A., Ramírez R., Andrés P., Andrés A., Ramírez R., Gómez-Lor B. 2009. Crystal structure and charge transport properties of N-trimethyltriindole: Novel p-type organic semiconductor single crystals. Organic Electronics 10 643–652.

Gruhn N. E., Silva Filho D. A., Bill T. G., Malagoli M., Coropceanu V., Kahn A., and Bre´das J. 2002. The Vibrational Reorganization Energy in Pentacene: Molecular Influences on Charge Transport. J. Am. Chem. Soc., 124, 7918-7919.

Huang W., Xie W., Huang H., Zhang H., and Liu H. 2020. Designing Organic Semiconductors with Ultrasmall Reorganization Energies: Insights from Molecular Symmetry, Aromaticity and Energy Gap. J. Phys. Chem. Lett., Just Accepted Manuscript.

Huong V. T. T., Nguyen H. T., Tai T. B., and Nguyen M. T. 2013. π-Conjugated Molecules Containing Naphtho[2,3-b]thiophene and Their Derivatives: Theoretical Design for Organic Semiconductors. J. Phys. Chem. C, 117, 10175−10184.

Hutchison G. R., Ratner M. A., and Marks T. J. 2005. Intermolecular Charge Transfer between Heterocyclic Oligomers. Effects of Heteroatom and Molecular Packing on Hopping Transport in Organic Semiconductors. J. Am. Chem. Soc., 127, 16866-16881.

Irfan A., Al-Sehemi A. G., Aijaz Rasool Chaudhry A. R., Muhammad S. 2018. The structural, electro-optical, charge transport and nonlinear optical properties of oxazole (4Z)-4-Benzylidene-2-(4-methylphenyl)-1,3-oxazol- 5(4H)-one derivative. Journal of King Saud University – Science 30, 75–82.

Jia X., Wei H., Shi Y., Liu Y. 2019. Theoretical studies on charge transport and optical properties of diarylmaleic anhydride derivatives as organic light-emitting materials. Chemical Physics Letters 724 50–56.

Köse M. E., Mitchell W. J., Kopidakis N., Chang C. H., Shaheen S. E., Kim K., and Rumbles G. 2007. Theoretical Studies on Conjugated Phenyl-Cored Thiophene Dendrimers for Photovoltaic Applications. J. AM. CHEM. SOC., 129, 14257-14270.

Krishna G. R., Devarapalli R., Lal G., and Reddy C. M. 2016. Mechanically Flexible Organic Crystals Achieved by Introducing Weak Interactions in Structure: Supramolecular Shape Synthons. J. Am. Chem. Soc., 138, 13561−13567.

Li H X, Wang X F, Li Z F. 2012. Theoretical study of the effects of different substituents of tetrathiafulvalene derivatives on charge transport. Chin Sci Bull, 57: 4049-4056.

Liu Y., Sun X., Gahungu G., Qu X., Wang Y. and Wu Z. 2013. DFT/TDDFT investigation on the electronic structures and photophysical properties of phosphorescent Ir (III) complexes with conjugated/non-conjugated carbene ligands. J. Mater. Chem. C, 1, 3700.

McMahon D. P. and Troisi A. 2010. Evaluation of the External Reorganization Energy of Polyacenes. J. Phys. Chem. Lett., 1, 941–946.

Navamani K., Saranya G., Kolandaivel P. and Senthilkumar K. 2013. Effect of structural fluctuations on charge carrier mobility in thiophene, thiazole and thiazolothiazole based oligomers. Phys.Chem. Chem. Phys.15, 17947.

Nguyen T. P., Shim J. H., and Lee J. Y. 2015. Density Functional Theory Studies of Hole Mobility in Picene and Pentacene Crystals. J. Phys. Chem. C, Just Accepted Manuscript.

Reed A. E., Carpenter J. E., and Weinhold F. 2014. NBO Version 3.1, E. D. Glendening.

Senevirathna W., Daddario C. M., and Sauvé G. 2014. Density Functional Theory Study Predicts Low Reorganization Energies for Azadipyrromethene-Based Metal Complexes. J. Phys. Chem. Lett., 5, 935−941.

Siddiqui S. A., Al-Hajry A., and Al-Assiri M. S. 2016. Ab Initio Investigation of 2,20-Bis(4-trifluoromethylphenyl)- 5,50-Bithiazole for the Design of Efficient Organic Field-Effect Transistors. International Journal of Quantum Chemistry, 116, 339–345.

Swicka S. M., Zhua W., Mattaa M., Aldricha T. J., Harbuzaruc A., Navarretec J. T. L., Ortizc R. P., Kohlstedta K. L., Schatza G. C., Facchettia A., Melkonyana F. S., and Marks T. J. 2018. Closely packed, low reorganization energy π-extended postfullerene acceptors for efficient polymer solar cells. PNAS Latest Articles.

Tan Y., Casetti N. C., Boudouris B. W., and Savoie B. M. 2021. Molecular Design Features for Charge Transport in Nonconjugated Radical Polymers. J. Am. Chem. Soc., 143, 11994−12002.

Tripathi A., Prabhakar C. 2019. Optoelectronic and charge-transport properties of truxene, isotruxene, and its heteroatomic (N, O, Si, and S) analogs: A DFT study. J Phys Org Chem.; 32: e3944.

Wang C., Dong H., Jiang L. and Hu W. 2018. Organic semiconductor crystals. Chem. Soc. Rev., ,47, 422.

Wang L., Duan G., Ji Y., and Zhang H. 2012. Electronic and Charge Transport Properties of peri- Xanthenoxanthene: The Effects of Heteroatoms and Phenyl Substitutions. J. Phys. Chem. C, 116, 22679−22686.

Wang L., Li T., Shen Y., and Song Y. 2016. A theoretical study of electronic structure and charge transport property for thieno[2,3-b] benzothiophene based derivatives. Phys. Chem. Chem. Phys. Qi Y., Chen C., Zheng C., Tang Y., Wan Y., Jiang H., Chen T., Tao Y. and Chen R. 2020. Heteroatom-bridged Heterofluorenes: A Theoretical Study on Molecular Structures and Optoelectronic Properties Phys. Chem. Chem. Phys., 00, 1-3.

Yan L., Zhao Y., Yu H., Hu Z., He Y., Li A., Goto O., Yan C., Chen T., Chen R., Loo L., Perepichka D., Meng H. and Huang, W.J. 2013. Influence of Heteroatoms on the Charge Mobility of Anthracene Derivatives. J. Name., 00, 1-3 | 1.

Yang L., Mao J., Yin C., Mohamad A. A., Wu X., Dong C., Liu Y., Wei Y., Xie L., Ran X. and Huang W. 2019. Novel Structure of Grid Spirofluorene: A New Organic Semiconductor with Low Reorganization Energy. J. Name., 2013, 00, 1-3 | 1.

Yang X., Wang L., Wang C., Long W., and Shuai Z. 2008. Influences of Crystal Structures and Molecular Sizes on the Charge Mobility of Organic Semiconductors: Oligothiophenes. Chem. Mater., Vol. 20, No. 9.

Zhang D., Xu F., Lu Q., Zhang R., Xia J. 2023. Poly(3-amino-carbazole) derivatives containing 1,10-phenanthroline and 8-hydroxyquinoline ligands: Synthesis, properties and application as ion sensors. Spectrochimica Acta Part A: Molecular and Biomolecular Spectroscopy, Vol. 295.

Zhang M. and Zhao G. 2012. Heteroatomic Effects on Charge-Transfer Mobility of Dianthra [2,3-b:2′,3′-f] thieno[3,2-b] thiophene (DATT) and Its Derivatives. J. Phys. Chem. C, 116, 19197−19202.

Zhu R., Duan Y., Geng Y., Wei C., Chen X., Liao Y. 2016. Theoretical evaluation on the reorganization energy of five-ring-fused benzothiophene derivatives. Computational and Theoretical Chemistry 1078 16–22.

Zhang Y., Cai X., Bian Y., Li X., and Jiang J. 2008. Heteroatom Substitution of Oligothienoacenes: From Good p-Type Semiconductors to Good Ambipolar Semiconductors for Organic Field-Effect Transistors. J. Phys. Chem. C, 112, 5148-5159.

Ajayi, International Journal of Science Letters (IJSL). 2024. 6(1): 377-410
https://doi.org/10.38058/ijsl.1319471

Research Article

Genetic variation, genotype × environment interaction, and correlation among drought tolerance indices in cowpea

Abiola Toyin Ajayi

Plant Breeding Unit, Department of Plant Science and Biotechnology, Adekunle Ajasin University, Akungba-Akoko, Nigeria

*Correspondence: toyin.ajayi@aaua.edu.ng

Abstract

Drought tolerance indices are valuable indicators for selecting cowpea genotypes with improved drought tolerance. However, there is a limited understanding of the variability and the impact of genotype (G) × environment (E) interaction (I) on these drought tolerance indices. Therefore, the objective of this study was to assess the extent of genetic variability and the influence of GEI on drought tolerance indices in cowpeas. The experiment was conducted over two seasons under controlled conditions in a screen house. The results revealed that seed yield and all drought tolerance indices were significantly influenced by genotype, environment, and GEI. When the data from both years were combined, the yield under non-stress conditions ranged from 10.47 g in G2 to 17.27 g in G7, while under drought stress, it ranged from 2.19 g in G3 to 6.89 g in G1. Through mean rank analysis, principal component (PC) analysis, and clustering, highly tolerant accessions (G1 and G6) and highly susceptible ones (G2, G3, and G8) were identified. This study identified several indices, including geometric mean (GM), yield index (YI), mean productivity (MP), stress tolerance index (STI), modified stress tolerance index for non-stress (MST1), and stress (MST2), GMP, and HM, as effective in selecting high-yielding and drought-tolerant accessions under non-stress and drought conditions. Additionally, the drought resistance index (DRI) and yield stability index (YSI) were reliable indicators under drought stress. Most of the indices exhibited moderate (≥ 30%) to high heritability (≥ 60%) and high genetic advance (≥ 20%), except for MST2, which had low heritability (12.73%).

Article History

Received 24.06.2023
Accepted 17.02.2024

Keywords

Genotypic correlations,
Heritability,
Stability,
Non-stress,
Drought stress

1. Introduction

Cowpea (*Vigna unguiculata* L. Walp) plays a critical role in food security in Nigeria and other tropical and subtropical countries in Africa and the world. Its role can never be over-emphasized

regarding capacity for soil replenishment, plasticity nature, influence on livestock and human nutrition, and income-earning (Ajayi et al., 2022). According to FAOSTAT (2020), production in Nigeria stood at 2.61 MT/annum (36% of worldwide production), out of 7.23 MT/annum produced worldwide. However, 94.9% of the total production worldwide comes from Africa. Despite its potential to guarantee food security in the face of climate change, it is one of the major crops being threatened by the consequences of climate change (de Nóvoa Pinto et al., 2021). This is reflected in its grain yield across Africa which falls far below the expected mark due to production constraints which can be biotic and abiotic (Adetumbi et al., 2020).

Drought is a major abiotic constraint and one of the consequences of climate change responsible for about 60% of crop failures attributed to climate disasters (Lao et al., 2022). Cultivation of cowpeas in tropical countries is majorly done under the rainfed system. However, tropical climate is majorly characterized by strong and unpredictable variations in rainfall patterns that can lead to water deficit with dire consequences for crop production. Drought has been reported as a recurrent phenomenon in tropical regions across the world, and it is projected to worsen in the future (Nauditt et al., 2022). In recent times, the complete failure of cowpea and other crops is not uncommon in several instances due to the increase in the prevalence of drought (Ajayi, 2020). As a result, solutions for combating the threat of drought stress to cowpea production in tropical regions must be established.

Deployment of strategies such as the introduction of drought-tolerant varieties, appropriate cultural practices, and suitable mechanization may alleviate the effect of climate change-driven drought on crop productivity (Bennani et al., 2017). However, the most cost-effective measure among these is access to drought-tolerant varieties. Hence, the urgency to develop superior cowpea genotypes with enhanced drought tolerance is a cost-effective method to address the impact of drought on the crop. Drought tolerance is a complex trait driven by various morphological and physiological traits. Therefore, selecting desirable genotypes in a breeding scheme requires an efficient screening technique (Bennani et al., 2017). Selection solely dependent on yield may automatically encompass several factors that contribute positively to drought tolerance. Nevertheless, variation and heritability for seed yield are low, especially under moisture deficit conditions (Ajayi, 2020). Furthermore, cowpea yield is highly influenced by genotype × environment interaction (GEI), hence selection must be based on the stability of performance across multiple environments (Ajayi et al., 2022).

Various drought tolerance indices have recently become pointers on which the selection of drought-tolerant genotypes of several crops can be made. These indices quantify tolerance based on calculated relationships between yield performance in drought stress and non-stress conditions (Bennani et al., 2017). Some of the most popular among these indices include geometric mean productivity (GMP), harmonic mean (HM), mean productivity (MP), stress tolerance index (STI), yield index (YI), yield stability index (YSI), drought resistance index (DRI), modified stress tolerance index for non-stress condition (MST_1), stress condition (MST_2). Al-Rawi (2016) identified different classes of tolerance among wheat genotypes. Those that were stable in non-

stress and stress conditions with lower reduction of yield by stress, and those with high yield only under non-stress conditions, and proposed GMP, STI, MP, HM, K_2STI (MST_2), and K_1STI (MST_1) as the most appropriate indices for selecting drought-tolerant genotypes. However, Ajayi (2020) proposed the combination of STI, GMP, MP, DRI, YSI, and YI, while Batieno et al. (2016) proposed STI, MP, and GMP in cowpea. Nonetheless, while these drought tolerance indices have become the key contributors to the breeding of drought-tolerant genotypes of crop species, the genetic variability and the effect of genotype by the environment interaction (GEI) on these indices have not been seriously explored. Therefore, information regarding the variability and GEI of drought tolerance indices in pinpointing cowpea genotypes with extraordinary stability for drought tolerance across different environments is a prerequisite in the breeding program of the crop. Taking cognizance of these, the objectives of the present study were:

i. To investigate the genetic variation and the effect of GEI on drought tolerance indices of cowpeas in two seasons.

ii. To assess the level of genotypic correlations among drought tolerance indices and seed yield in cowpeas.

iii. To introduce a new drought tolerance index (intensity of drought resistance, IDR), and compare its strength with the existing ones in selecting drought-tolerant genotypes of cowpea.

2. Materials and Methods

2.1 Plant materials

Ten accessions of cowpeas used for the present study were chosen based on their high yields and early flowering. The seeds of these accessions were sourced from the International Institute of Tropical Agriculture (IITA), Nigeria. Nine out of these accessions had previously been screened for drought tolerance at different stages. The accessions with their countries of origin and drought tolerance at the seedling and the vegetative stages (Ajayi et al., 2018; Ajayi et al., 2020) are presented in Table 1.

Table 1. List of accessions and their countries of origin

S/N	Accession ID	Country of origin	Seedling stage	Vegetative stage	Code
1	TVu-763	Ghana	-	-	G1
2	TVu-207	USA	Drought tolerant	Moderately tolerant	G2
3	Tvu-218	USA	Highly susceptible	Highly susceptible	G3
4	Tvu-235	Ghana	Drought tolerant	Moderately tolerant	G4
5	Tvu-236	Ghana	Moderately tolerant	Moderately tolerant	G5
6	Tvu-241	USA	Drought tolerant	Drought tolerant	G6
7	IT98K-205-8	Nigeria	Moderately tolerant	Drought tolerant	G7
8	IT98K-555-1	Nigeria	Highly susceptible	Highly susceptible	G8
9	Tvu-4886	Niger	Moderately tolerant	Moderately tolerant	G9
10	Tvu-9256	Burkina Faso	Highly susceptible	Highly susceptible	G10

2.2 Experimental environment and methods

The experimental site was located within Adekunle Ajasin University, Akungba-Akoko, at 7.20° N Latitude, and 5.44'E Longitude at 423 m above sea level. The experiment was conducted over two years in 2019 and 2021 between March and July. The accessions were assessed in plastic pots (5 L each with three perforations beneath for draining excess moisture) laid out in a completely randomized design (CRD) in three replicates for drought stress and non-stress treatments in the screen house of the Department of Plant Science and Biotechnology. Each pot contained 3.5 kg of sieved top soil which was sown with ten seeds per accession in each replicate. Each replicate consisted of five pots per accession, totaling one hundred and fifty pots for each drought stress and non-stress treatment. Two weeks after emergence, seedlings were thinned to two plants per pot. One hundred percent (100%) field capacity of the soil per pot was predetermined at approximately 250 ml according to (Ogbaga et al., 2014). Each plastic pot for the non-stress treatment was watered to 100% field capacity every other day for five weeks after which watering was applied daily till the termination of the experiment. The pots for the drought stress treatment were taken to 100% field capacity once per week till the end of the experiment.

2.3 Data collection and analyses

At maturity, pods were harvested and threshed; and seed yield was determined per plant for each accession per treatment in each year. Ten already existing drought tolerance indices and a new one (intensity of drought resistance, IDR) were adopted for each accession based on the yield per plant in the non-stress and drought stress treatment. The drought tolerance indices are as follows:

i. Intensity of drought resistance (IDR) = $\frac{Ys/Yp}{\bar{Y}s}$ (Newly formulated)

ii. Geometric mean productivity (GMP) = $\sqrt{Yp \times Ys}$ (Kristin et al., 1997)

iii. Harmonic mean (HM) = $\frac{2(Yp \times Ys)}{Yp+Ys}$ (Kristin et al., 1997)

iv. Mean productivity (MP) = $\frac{Yp+Ys}{2}$ (Rosielle and Hamblin, 1981)

v. Stress tolerance index (STI) = $\frac{(Ys)(Yp)}{(\bar{Y}p)^2}$ (Fernadez, 1992)

vi. Yield index (YI) = $\frac{Ys}{\bar{Y}s}$ (Gavuzzi et al., 1997)

vii. Yield stability index (YSI) = $\frac{Ys}{Yp}$ (Bouslama and Schapaugh, 1984)

viii. Drought resistance index (DRI) = $Ys \times (\frac{Ys}{Yp})/\ \bar{Y}p$ (Moosevi et al., 2008)

ix. Modified stress tolerance index for the non-stress conditions (MST_1) = K_1STI (Farshadfar and Sutka, 2002)

   a. $K_1 = \frac{Yp^2}{\bar{Y}p^2}$ for non-stress treatment

x. Modified stress tolerance index for stress conditions (MST_2) = K_2STI (Farshadfar and Sutka, 2002)

   a. $K_2 = \frac{Ys^2}{\bar{Y}s^2}$ for drought stress treatment

Where, *Yp*, *Ys*, $\bar{Y}p$, and $\bar{Y}s$ were the mean seed yield of an accession under non-stress, mean grain yield in stress treatment, mean seed yield for all accessions in non-stress, and mean grain yield for all accessions in stress treatment, respectively. Possession of a higher value of any of the drought tolerance indices meant higher desirability, hence a higher level of drought tolerance.

All data were analyzed statistically. Individual ANOVA and mean separation (using DMRT at $P \leq 0.05$) were done for each year with version 20 of SPSS, followed by combined ANOVA for the two years. ANOVA was performed using the GLM procedure of SPSS, where the environment (year) was regarded as a fixed factor while genotype (accession) and treatment were random factors. Principal Component Analysis (PCA), biplot, and cluster analysis were assessed with PAST version 4.01 (Hammer et al., 2001). The genotypic correlation was done with the Plant Breeding Tools version 1.4 (PBTools, 2014) for each year and the coefficient was compared alongside the "t" table correlation values ($P \leq 0.05$; $P \leq 0.01$) at df = n–2 (Fisher and Yates, 1963).

Estimates of genetic parameters were performed as follows:

Error variance (*Ve*) = σ_e^2 = Mean square error (MSe)
Genotype × environment variance (V_{GE}) = $\sigma_{GE}^2 = (MS_{GE} - MS_e)/r$
Genotypic variance (V_G) = $\sigma_G^2 = (MS_G - MS_e)/re$
Phenotypic variance (V_P) = $V_G + V_{GE}/e + V_e/re$ (Songsri et al., 2008)
Genotypic coefficient of variation (*GCV*) = $\frac{\sqrt{V_G}}{\bar{X}} \times 100$
Phenotypic coefficient of variation (*PCV*) = $\frac{\sqrt{V_P}}{\bar{X}} \times 100$
Broad-sense heritability (H^2) = $V_G/(V_G + (V_{GE}/e) + (V_e/re))$ (Badu-apraku et al., 2021)
Genetic advance (GA) = $\frac{VG}{\sqrt{VP}} \times k$; k = 2.06 (selection differential) (Fayeun et al., 2016)

Genetic advance as percent of the mean (GAM) = $\frac{GA}{\bar{\chi}} \times 100$; where e, $\bar{X}$, and r are the number of environments, grand mean of trait, and replicates within environments, respectively. Genetic parameters were categorized according to Ajayi et al. (2014).

Stability = V_{GE}/V_G (Hossain et al., 2013).

3. Results

Combined ANOVA for seed yield showed that the effect of accession (genotype), treatment, and their interactions was highly significant (Table 2). Combined ANOVA for seed yield under differential drought conditions and drought tolerance indices showed a highly significant accession (genotype), year (environment), and accession (genotype) × year (environment) effect (Table 3).

Table 2. Mean squares values from combined ANOVA for seed yield per plant of ten accessions of cowpeas evaluated under differential drought stress in 2019 and 2021

Source of variation	Degree of freedom	Seed yield per plant
Accession	9	49.39
Treatment	1	1703.31
Year	1	1663.92
Accession × Treatment	9	20.79
Accession × Year	9	37.97
Treatment × Year	1	379.15
Accession × Treatment × Year	9	19.63
Error	18	0.52

All sources of variation are significant at P≤0.05

Table 3. Mean square values from combined ANOVA for seed yield and drought tolerance indices of ten accessions of cowpeas evaluated under differential drought stress in 2019 and 2021

Source of variation	Df	Yp (g)	Ys (g)	ReY (%)	IDR	GMP	HM	MP	STI	YI	YSI	DRI	MST_1	MST_2
Accession	9	27.94	14.16	1254.50	0.01	12.02	15.81	10.66	0.44	0.67	0.13	0.06	13.34	15.50
Year	1	1815.82	227.26	771.96	0.26	602.60	450.66	831.96	0.28	0.29	0.08	0.02	28.70	32.25
Accession × Year	9	45.08	12.52	594.67	0.01	17.54	17.98	18.99	0.54	0.57	0.06	0.03	13.39	105.24
Error	40	4.69	0.59	134.52	0.002	1.01	0.82	1.49	0.01	0.02	0.01	0.01	0.46	0.16

All the sources of variations are significant at P≤0.05

Df: Degree of freedom; Yp: Yield under non-stress condition; Ys: Yield under stress condition; ReY: Percent reduction in yield; IDR: Intensity of drought resistance; GMP: Geometric mean productivity; HM: Harmonic mean; MP: Mean productivity; STI: Stress tolerance index; YI: Yield index; YSI: Yield stability index; DRI: Drought resistance index; MST_1: Modified stress tolerance index for the non-stress conditions; MST_2: Modified stress tolerance index for stress conditions.

The mean performances of accessions across treatments and years for yield and drought tolerance indices are presented in Table 4 (a–c). In 2019, the mean seed yield under non-stress and stress conditions respectively was 17.76 g and 6.67 g, however, the mean seed yield in 2021 under non-stress and stress conditions respectively was 6.76 g and 2.78 g while that for the combined drought stress and non-stress conditions respectively, was 12.26 g and 4.72 g. Therefore, a reduction due to drought stress in 2019, 2021, and the combined years respectively, was 60.81, 53.63, and 57.22%; the highest percentage reduction in yield (79.48%) under drought stress for the combined seasons was observed in accession G3. Furthermore, accessions G7 and G8 exhibited a consistent above-average reduction in yield across the years. Accessions G10 and G9 consistently had above-average performance under both conditions in 2019, accessions G7 and G6 performed above average in both conditions in 2021, while accessions G10 and G6 had an above-average performance under both conditions for the combined season, and no single accession had the best performance under both conditions across the years. In 2019, accessions G1, G9, and G5 had an above-average performance for all the drought tolerance indices, G10, and G6 were next in line. The values ranged from the lowest (0.02) in MST_1 to the highest (12.22) in MP. However, in 2021, accessions G6 and G7 were the only above-average performing accessions for such indices as GMP (4.26), HM (3.82), MP (4.77), STI (0.51), YI (1.14), DRI (0.20), MST_1 (1.41), and MST_2 (1.53). Nevertheless, accession G6 was the only above-average performing accession for all indices for the combined season which means ranged from the lowest (0.12) in IDR to the highest (8.49) in MP. Stability was nonetheless very high in GMP (0.74), ReY (0.82), and HM (0.87), but moderate in YSI (1.00), while other parameters were highly unstable ($\sigma^2g\times e/\sigma^2g > 1.0$).

The ranking of accessions for the determination of the most desirable drought-tolerant accessions based on all the drought tolerance indices is presented in Table 5. Accessions G1 and G6 which exhibited the lowest rank sum and rank means, and around the average standard deviation of rank were the most drought-tolerant accessions. These were followed by accessions G7, G9, and G10, which exhibited a combination of below-average rank sum, rank means, and above-average standard deviation of rank, and G5 which exhibited slightly below-average rank sum and the least standard deviation of rank (1.37) as moderately drought tolerant accession, while accessions G2, G3, G4, and G8 with the highest rank sum and rank means were the most drought susceptible accessions under drought stress. Cluster analysis (Figure 1) using the unweighted pair group method with arithmetic mean (UPGMA) classified the accessions into three major clusters based on their similarities for drought tolerance indices. Cluster I consisted of G8, G3, and G2 which exhibited low drought tolerance indices consistently across years with below-average tolerance indices for the combined seasons and thus were the most susceptible accessions. Cluster II, sub-cluster A consisted only of G6, a highly tolerant accession with above-average HM, YI, and DRI across years and above-average performance for all the drought tolerance indices for the combined seasons; while sub-cluster B consisted of G7, and G4, moderately tolerant and moderately susceptible accessions exhibiting around average to above average drought tolerance indices across years and for the combined seasons. Cluster III, sub-cluster A consisted of only G1, a highly tolerant accession exhibiting above-average IDR, YSI, DRI, and MST_1 consistently across years,

and above-average performance for all drought tolerance indices except MST_1 and MST_2 for the combined seasons; while sub-cluster B consisted of G10, G9, and G5, which are moderately-tolerant accessions exhibiting high GMP, HM, MP, STI, YI, MST_1, and MST_2 in 2019 and below-average values for most drought tolerance indices in 2021.

The combined estimates of genetic parameters of yield and drought tolerance indices are presented in Table 6. GCV was high in all parameters except for yield under non-stress conditions, GMP, and MP which were moderate, with a range of between 14.57 percent in MP and 203.65 percent in MST_1. PCV on the other hand was high for all parameters and ranged from the lowest (20.44%) in MP to the highest (224.38%) in MST_1. However, the differences between GCV and PCV for most parameters were also high. Broad sense heritability was low (12.73%) in MST_2 and moderate for other parameters except for ReY, DRI, and YSI, which exhibited high heritability. Nevertheless, GAM was high for all parameters and ranged from the lowest (21.39%) in MP to the highest (399.71%) in MST_2.

The Principal Component Analysis (PCA) of the measured parameters is presented in Table 7. In each year, there were two PC axes whose eigenvalues exceeded 1.0 and also accounted for more than 98 percent of the total variation. However, the combined seasons possessed three PC axes whose eigenvalues exceeded 1.0 contributing more than 98 percent of the total variation. In the 2019 season, all parameters had a high contribution (≥ 0.50) to the total variation in PC1 except for yield under non-stress conditions, in contrast to PC2 where they all had low contributions except for yield in non-stress conditions, DRI, IDR, and MST_2. However, in the 2021 season, all parameters had high contributions in PC1 except for the percent reduction in yield, DRI, and STI, while only ReY, DRI, STI, and MST_1 were the only significant contributors in PC2. Nonetheless, in the combined seasons, all parameters were high contributors in PC1 except seed yield in non-stress conditions while the major contributors in PC2 included yield in non-stress conditions, ReY, IDR, STI, MST_1, MST_2, and YSI. The contributions ranged from the lowest (0.09) in yield under non-stress conditions to the highest (0.99) in yield under drought stress, HM, and MP in PC1, while it ranged from the lowest (0.06) in HM to the highest (0.98) in yield under non-stress in PC2 for 2019. However, ranges between 0.20 (DRI) to 0.99 (GMP, HM, and MP) for PC1, and 0.0003 (MST2) to 0.98 (ReY, DRI, and STI) for PC2 were observed in 2021 while the combined seasons exhibited ranges between 0.28 in yield under non-stress conditions and 0.98 in HM and YI for PC1, between 0.09 in HM and 0.73 in MST_1 for PC2, and between 0.02 in HM and 0.62 in yield under non-stress conditions for PC3.

The biplots derived from the PCA for 2019, 2021, and combined seasons, respectively are presented in Figures 2 – 4, while Figures 5 – 7 present the polygon views of the biplots showing the vertex accessions for 2019, 2021, and the combined seasons respectively. In 2019, quadrant I contained the moderately tolerant accessions: G10 and G9; quadrant II contained the highly tolerant accessions: G1 and G6, and a moderately tolerant G5; quadrant III contained the highly susceptible accessions: G3, G8, and G2; while quadrant IV contained the moderately tolerant accessions: G7 and G4. Parameters such as HM, MST_2, GMP, and STI were positively correlated

in the upper part of quadrant I, while yield under non-stress, MST_1, and MP were also positively correlated in the lower part of quadrant I. The vertex accession in quadrant I for yield under non-stress, MST_1, and MP was G10. Yield under drought stress, YI, DRI, YSI, and IDR were positively correlated in quadrant II with the vertex accessions being G1 and G6. In 2021 however, quadrants I and II respectively contained G6, highly tolerant accession, and G7, moderately tolerant. Parameters such as yield under drought stress, YI, HM, and MST_2 were highly positively correlated at the base of quadrant I and also correlated positively with MST_1, GMP, MP, and seed yield under non-stress which were highly positively correlated at the upper quadrant II. The only vertex accession for these parameters is G6. Quadrant III contained the most susceptible accessions; G8, G3, and G2, with the vertex being G3 and G2. Quadrant IV contained highly tolerant accession: G1, and moderately tolerant accessions: G5, G4, G10, and G9. Parameters such as IDR and YSI were highly correlated in quadrant IV with vertex accession being G9. In the combined seasons nonetheless, quadrant I contained the highly tolerant G6 and the moderately tolerant G7, and quadrant II contained the moderately tolerant G10, G5, G9, and the highly tolerant G1. Quadrant III contained the highly susceptible G8, G2, and the moderately tolerant G4 while quadrant IV contained the G3, the most susceptible accession. MST_1, MST_2, STI, and MP were highly positively correlated with yield under non-stress conditions in quadrant I with the vertex accessions being G7 highly correlating with yield under non-stress and G6 highly correlating with indices such as MST_1, MST_2, STI, and MP. YI, GMP at the base of quadrant I with HM, DRI, YSI, and IDR in quadrant II were highly positively correlated with seed yield under drought stress conditions with the vertex accession being G9. While the only parameter linked to quadrant IV was the percentage reduction in yield (ReY) correlating with the vertex accession G3, the most susceptible accession to drought, no parameter was linked to quadrant III where G2 was the vertex accession.

The genotypic correlation between drought tolerance indices and yield under non-stress and drought-stress conditions for the two years is presented in Table 8. MST_1 consistently was positively correlated with seed yield under drought stress (0.71* and 0.95**) and non-stress (0.65* and 0.91**) conditions across the years. MP had a consistent positive correlation with yield for the non-stress condition for 2019 (0.76**) and 2021 (0.99**). However, yield under stress conditions consistently had a positive correlation across years with indices such as DRI (0.97** and 0.79**), GMP (0.91**, 0.95**), HM (0.98**), YI (1.00**), STI (0.92**, 0.95**), and MST_2 (0.97**, 0.93**).

Table 4a. Mean performance for seed yield per plant and drought tolerance indices of ten accessions of cowpeas evaluated under differential drought stress in 2019 and 2021

Accession	Yp (g)	Ys (g)	ReY (%)	IDR	GMP	HM	MP	STI	YI	YSI	DRI	MST_1	MST_2
G1	16.17^{a}	11.19^{e}	30.63^{a}	0.10^{d}	13.45^{d}	13.23^{f}	13.69^{cde}	0.58^{c}	1.68^{e}	0.69^{d}	0.44^{f}	0.03^{bc}	0.15^{d}
G2	15.66^{ab}	6.34^{cd}	59.39^{c}	0.06^{b}	9.96^{bc}	9.02^{cd}	10.99^{abc}	0.32^{ab}	0.95^{cd}	0.41^{b}	0.14^{bcd}	0.02^{ab}	0.05^{ab}
G3	14.49^{ab}	2.54^{a}	82.32^{d}	0.03^{a}	6.04^{a}	4.30^{a}	8.52^{a}	0.11^{a}	0.38^{a}	0.18^{a}	0.03^{a}	0.01^{a}	0.01^{a}
G4	20.35^{bc}	3.78^{ab}	81.25^{d}	0.03^{a}	8.76^{b}	6.37^{b}	12.07^{bcd}	0.24^{ab}	0.57^{ab}	0.19^{a}	0.04^{ab}	0.02^{ab}	0.02^{a}
G5	17.35^{ab}	7.78^{d}	53.89^{bc}	0.07^{bc}	11.59^{cd}	10.69^{de}	$12.57^{b\text{-}e}$	0.43^{bc}	1.17^{d}	0.46^{bc}	0.20^{cd}	0.02^{abc}	0.08^{bc}
G6	13.46^{a}	7.33^{d}	45.03^{b}	0.08^{c}	9.91^{bc}	9.46^{cd}	10.39^{ab}	0.31^{ab}	1.09^{d}	0.55^{c}	0.23^{d}	0.01^{ab}	0.05^{ab}
G7	23.61^{c}	4.76^{bc}	80.01^{d}	0.03^{a}	10.59^{bc}	7.91^{bc}	14.19^{de}	0.36^{b}	0.71^{bc}	0.19^{a}	0.05^{ab}	0.03^{abc}	0.04^{ab}
G8	14.90^{a}	5.06^{bc}	66.11^{c}	0.05^{b}	8.68^{b}	7.55^{bc}	9.98^{ab}	0.24^{ab}	0.76^{bc}	0.34^{b}	0.09^{abc}	0.01^{ab}	0.03^{ab}
G9	18.64^{abc}	10.06^{e}	44.09^{b}	0.08^{c}	13.53^{d}	12.79^{ef}	14.35^{de}	0.58^{c}	1.51^{e}	0.56^{c}	0.33^{e}	0.03^{bc}	0.13^{d}
G10	22.96^{c}	7.86^{d}	65.36^{c}	0.05^{b}	13.42^{d}	11.69^{ef}	15.41^{e}	0.59^{c}	1.18^{d}	0.35^{b}	0.15^{bcd}	0.05^{c}	0.11^{cd}
$\bar{X}$	**17.76**	**6.67**	**60.81**	**0.06**	**10.59**	**9.30**	**12.22**	**0.38**	**1.00**	**0.39**	**0.17**	**0.02**	**0.07**
Minimum	11.62	2.16	26.74	0.02	5.83	3.80	7.85	0.11	0.32	0.14	0.02	0.004	0.01
Maximum	29.58	12.10	86.34	0.11	16.49	14.03	19.39	0.86	1.81	0.73	0.50	0.08	0.18
LSD (0.05)	4.01	1.43	10.56	0.01	1.91	1.70	2.31	0.14	0.19	0.11	0.09	0.01	0.02
CV (%)	16.08	15.29	12.37	16.67	12.84	13.04	13.45	26.32	14.14	19.86	37.20	50.00	45.18

Mean values accompanied by the same superscript in a column are not significantly different from one another at $P \leq 0.05$ using DMRT. $\bar{X}$: Grand mean; LSD: Least significant difference; CV: Coefficient of variation; Yp: Yield under non-stress condition; Ys: Yield under stress condition; ReY: Percent reduction in yield; IDR: Intensity of drought resistance; GMP: Geometric mean productivity; HM: Harmonic mean; MP: Mean productivity; STI: Stress tolerance index; YI: Yield index; YSI: yield stability index; DRI: Drought resistance index; MST_1: Modified stress tolerance index for the non-stress condition; MST_2: Modified stress tolerance index for stress condition.

Table 4b. Mean performance for seed yield per plant and drought tolerance indices of ten accessions of cowpea evaluated under differential drought stress in 2021

Accession	Yp (g)	Ys (g)	ReY (%)	IDR	GMP	HM	MP	STI	YI	YSI	DRI	MST_1	MST_2
G1	5.13^{ab}	2.58^{bc}	49.29^{a-d}	0.21^{b-e}	3.63^{bc}	3.42^{bc}	3.86^{ab}	0.31^{ab}	1.06^{bc}	0.51^{b-e}	0.20^{bc}	0.19^{a}	0.36^{a}
G2	5.28^{ab}	1.47^{a}	71.85^{de}	0.12^{ab}	2.79^{a}	2.30^{a}	3.38^{ab}	0.19^{a}	0.60^{a}	0.28^{ab}	0.06^{a}	0.13^{a}	0.07^{a}
G3	8.08^{c}	1.86^{ab}	76.65^{e}	0.09^{a}	3.86^{c}	3.01^{ab}	4.97^{c}	0.35^{ab}	0.76^{ab}	0.23^{a}	0.07^{ab}	0.56^{a}	0.20^{a}
G4	5.10^{ab}	3.04^{cd}	40.05^{ab}	0.25^{de}	3.94^{c}	3.81^{c}	4.07^{bc}	0.37^{b}	1.25^{cd}	0.59^{de}	0.28^{cd}	0.23^{a}	0.58^{a}
G5	4.92^{ab}	2.46^{bc}	45.76^{abc}	0.22^{cde}	3.45^{abc}	3.24^{bc}	3.69^{ab}	0.29^{ab}	1.01^{bc}	0.54^{cde}	0.20^{bc}	0.21^{a}	0.31^{a}
G6	14.31^{e}	5.75^{e}	59.47^{b-e}	0.17^{a-d}	9.06^{e}	8.19^{e}	10.03^{e}	1.95^{d}	2.35^{e}	0.41^{a-d}	0.36^{d}	9.61^{c}	10.80^{c}
G7	10.94^{d}	3.68^{d}	65.52^{cde}	0.14^{abc}	6.28^{d}	5.43^{d}	7.31^{d}	0.94^{c}	1.51^{d}	0.34^{abc}	0.21^{bc}	2.64^{b}	2.33^{b}
G8	6.36^{bc}	1.95^{ab}	69.02^{cde}	0.13^{abc}	3.49^{abc}	2.96^{ab}	4.15^{bc}	0.29^{ab}	0.79^{ab}	0.31^{abc}	0.09^{ab}	0.32^{a}	0.22^{a}
G9	3.33^{a}	2.48^{bc}	24.68^{a}	0.31^{e}	2.87^{ab}	2.83^{ab}	2.90^{a}	0.19^{ab}	1.02^{bc}	0.75^{e}	0.29^{cd}	0.05^{a}	0.20^{a}
G10	4.14^{a}	2.49^{bc}	34.05^{a}	0.27^{e}	3.17^{abc}	3.03^{ab}	3.32^{ab}	0.24^{ab}	1.02^{bc}	0.66^{e}	0.26^{cd}	0.11^{a}	0.25^{a}
$\bar{X}$	**6.76**	**2.78**	**53.63**	**0.19**	**4.26**	**3.82**	**4.77**	**0.51**	**1.14**	**0.46**	**0.20**	**1.41**	**1.53**
Minimum	6.00	5.94	80.24	0.40	9.52	8.37	10.83	2.15	2.43	11.60	0.42	13.01	11.60
Maximum	2.84	1.35	2.22	0.08	2.44	2.07	2.67	0.14	0.55	0.04	0.05	0.40	0.04
LSD (0.05)	1.54	0.53	18.41	0.08	0.59	0.58	0.76	0.13	0.24	0.79	0.11	1.34	0.79
CV (%)	16.27	13.46	24.45	28.83	9.96	10.79	11.29	17.54	15.19	30.74	38.73	67.66	36.97

Mean values accompanied by the same superscript in a column are not significantly different from one another at $P \leq 0.05$ using DMRT. **$\bar{X}$**: Grand mean; LSD: Least significant difference; CV: Coefficient of variation; Yp: Yield under non-stress condition; Ys: Yield under stress condition; ReY: Percent reduction in yield; IDR: Intensity of drought resistance; GMP: Geometric mean productivity; HM: Harmonic mean; MP: Mean productivity; STI: Stress tolerance index; YI: Yield index; YSI: yield stability index; DRI: Drought resistance index; MST_1: Modified stress tolerance index for the non-stress condition; MST_2: Modified stress tolerance index for stress condition.

Table 4c. Combined mean performance for seed yield per plant and drought tolerance indices of ten accessions of cowpea evaluated under differential drought stress in 2019 and 2021

Accession	Yp (g)	Ys (g)	ReY (%)	IDR	GMP	HM	MP	STI	YI	YSI	DRI	MST_1	MST_2
G1	10.65^{a}	6.89^{e}	39.96^{ab}	$0.16d^{e}$	8.54^{de}	8.32^{fg}	8.77^{b}	0.44^{d}	1.37^{d}	0.60^{de}	0.32^{d}	0.11^{a}	0.25^{a}
G2	10.47^{a}	3.91^{b}	65.62^{d}	0.09^{abc}	6.38^{bc}	5.66^{bc}	7.19^{a}	0.25^{ab}	0.78^{b}	0.34^{b}	0.10^{ab}	0.07^{a}	0.06^{a}
G3	11.29^{ab}	2.19^{a}	79.48^{e}	0.06^{a}	4.95^{a}	3.66^{a}	6.74^{a}	0.23^{a}	0.57^{a}	0.21^{a}	0.05^{a}	0.28^{a}	0.11^{a}
G4	12.73^{abc}	3.41^{b}	60.65^{cd}	0.14^{cd}	6.35^{bc}	5.09^{b}	8.07^{ab}	0.31^{abc}	0.91^{b}	0.39^{bc}	0.16^{bc}	0.12^{a}	0.29^{a}
G5	11.13^{ab}	5.13^{cd}	49.83^{bc}	0.15^{d}	7.52^{cd}	6.97^{de}	8.13^{ab}	0.36^{bcd}	1.09^{c}	0.50^{cd}	0.20^{c}	0.12^{a}	0.19^{a}
G6	13.89^{c}	6.54^{e}	52.25^{bc}	0.12^{bcd}	9.49^{e}	8.82^{g}	10.21^{c}	1.13^{f}	1.73^{e}	0.48^{cd}	0.29^{d}	4.81^{c}	5.43^{c}
G7	17.27^{d}	4.22^{bc}	72.76^{de}	0.09^{ab}	8.44^{de}	6.67^{cd}	10.75^{c}	0.65^{e}	1.11^{c}	0.27^{ab}	0.13^{abc}	1.33^{b}	1.18^{b}
G8	10.63^{a}	3.50^{b}	67.56^{de}	0.09^{abc}	6.09^{b}	5.25^{b}	7.07^{a}	0.27^{ab}	0.78^{b}	0.32^{ab}	0.09^{ab}	0.16^{a}	0.13^{a}
G9	10.98^{a}	6.27^{e}	34.38^{a}	0.19^{e}	8.19^{d}	7.81^{efg}	8.62^{b}	0.39^{cd}	1.26^{cd}	0.66^{e}	0.31^{d}	0.04^{a}	0.17^{a}
G10	13.55^{bc}	5.18^{d}	49.70^{bc}	0.16^{de}	$8.29d^{e}$	7.36^{def}	9.36^{bc}	0.41^{cd}	1.10^{c}	0.50^{cd}	0.21^{c}	0.08^{a}	0.18^{a}
$\bar{X}$	**12.26**	**4.72**	**57.22**	**0.12**	**7.42**	**6.56**	**8.49**	**0.44**	**1.07**	**0.43**	**0.19**	**0.71**	**0.79**
Minimum	9.80	2.05	19.11	0.06	4.75	3.41	6.58	0.21	0.55	0.20	0.04	0.03	0.04
Maximum	18.78	7.42	80.23	0.24	9.88	9.20	11.70	1.21	0.81	0.81	0.44	6.51	5.82
LSD (0.05)	2.97	1.05	15.94	0.06	1.37	1.24	1.67	0.14	0.19	0.14	0.14	0.93	0.55
CV (%)	17.66	16.27	20.27	37.27	13.54	13.8	14.38	22.73	13.22	23.26	52.63	95.53	50.63

Mean values accompanied by the same superscript in a column are not significantly different from one another at $P \leq 0.05$ using DMRT. $\bar{X}$: Grand mean; LSD: Least significant difference; CV: Coefficient of variation; Yp: Yield under non-stress condition; Ys: Yield under stress condition; ReY: Percent reduction in yield; IDR: Intensity of drought resistance; GMP: Geometric mean productivity; HM: Harmonic mean; MP: Mean productivity; STI: Stress tolerance index; YI: Yield index; YSI: yield stability index; DRI: Drought resistance index; MST_1: Modified stress tolerance index for the non-stress condition; MST_2: Modified stress tolerance index for stress condition.

Table 5. The ranking of accessions of cowpeas evaluated under differential drought stress in 2019 and 2021 based on their superiority for seed yield and drought tolerance indices

Accession	Yp	Ys	ReY	IDR	GMP	HM	MP	STI	YI	YSI	DRI	MST_1	MST_2
	2019												
G1	6	1	1	1	10	1	4	3	1	1	1	3	1
G2	7	6	5	5	6	6	7	6	6	5	6	6	6
G3	9	10	10	10	2	10	10	10	10	10	10	10	10
G4	3	9	9	9	8	9	6	8	9	9	9	7	9
G5	5	4	4	4	4	4	5	4	4	4	4	5	4
G6	10	5	3	3	7	5	8	7	5	3	3	8	5
G7	1	8	8	8	5	7	3	5	8	8	8	4	7
G8	8	7	7	7	9	8	9	9	7	7	7	9	8
G9	4	2	2	2	1	2	2	2	2	2	2	2	2
G10	2	3	6	6	3	3	1	1	3	6	5	1	3
$\bar{X}$													

Yp: Yield under non-stress condition; Ys: Yield under stress condition; ReY: Percent reduction in yield; IDR: Intensity of drought resistance; GMP: Geometric mean productivity; HM: Harmonic mean; MP: Mean productivity; STI: Stress tolerance index; YI: Yield index; YSI: yield stability index; DRI: Drought resistance index; MST_1: Modified stress tolerance index for the non-stress condition; MST_2: Modified stress tolerance index for stress condition.

Table 5 contd.

Accession	Yp	Ys	ReY	IDR	GMP	HM	MP	STI	YI	YSI	DRI	MST_1	MST_2	*RS*	$\bar{R}$	*SDR*
								2021								
G1	6	4	5	5	5	4	6	5	4	5	6	7	4	100	**3.85**	**2.36**
G2	5	10	9	9	10	10	8	10	10	9	10	8	10	195	7.50	**1.94**
G3	3	9	10	10	4	7	3	4	9	10	9	3	8	210	8.08	2.86
G4	7	3	3	3	3	3	5	3	3	3	3	5	3	151	**5.81**	2.69
G5	8	7	4	4	7	5	7	7	7	4	7	6	5	133	**5.12**	**1.37**
G6	1	1	6	6	1	1	1	1	1	6	1	1	1	100	**3.85**	2.79
G7	2	2	7	7	2	2	2	2	2	7	5	2	2	124	**4.77**	2.64
G8	4	8	8	8	6	8	4	6	8	8	8	4	7	189	7.27	**1.46**
G9	10	6	1	1	9	9	10	9	6	1	2	10	9	110	**4.23**	3.46
G10	9	5	2	2	8	6	9	8	5	2	4	9	6	118	**4.54**	2.61
$\bar{X}$														143	5.502	2.418

RS: Rank sum; $\bar{R}$: Rank mean; SDR: Standard deviation of rank. $\bar{X}$: Grand mean; Yp: Yield under non-stress conditions; Ys: Yield under stress condition; ReY: Percent reduction in yield; IDR: Intensity of drought resistance; GMP: Geometric mean productivity; HM: Harmonic mean; MP: Mean productivity; STI: Stress tolerance index; YI: Yield index; YSI: yield stability index; DRI: Drought resistance index; MST_1: Modified stress tolerance index for the non-stress condition; MST_2: Modified stress tolerance index for stress condition.

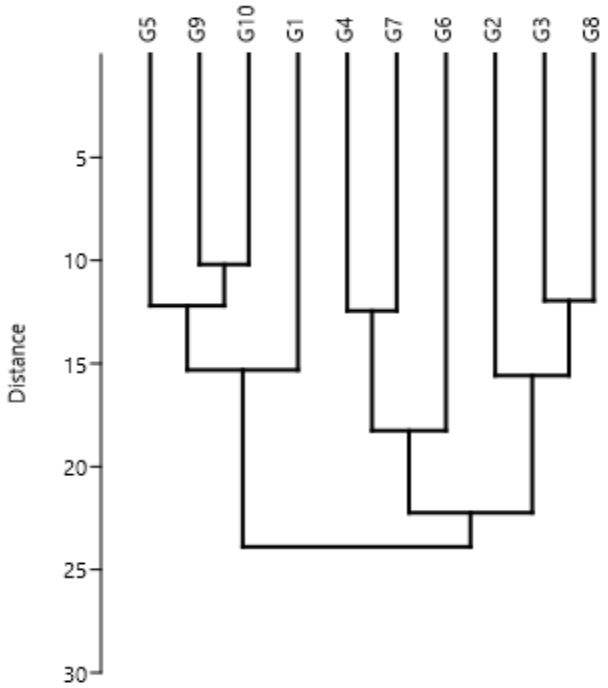

Figure 1. Dendrogram (UPGMA) shows the classification of accessions of cowpeas based on the ranking of their drought tolerance indices. G1 – G10 are codes for accessions of cowpea evaluated.

Table 6. Combined estimates of genetic parameters of seed yield and drought tolerance indices of ten accessions of cowpeas evaluated under differential drought stress in 2019 and 2021

Trait	Mean	σ^2g	σ^2ge	σ^2p	σ^2e	GCV (%)	PCV (%)	h^2B (%)	GAM (%)	Stability
Yp	12.26	3.88	13.46	8.57	4.69	16.06	23.88	34.06	22.27	3.46
Ys	4.73	2.26	3.99	2.83	0.59	31.78	35.57	52.07	58.51	1.77
ReY	57.22	186.66	153.38	321.18	134.52	23.88	31.34	65.32	37.49	**0.82**
DRI	0.19	0.008	0.01	0.018	0.01	47.08	70.61	60.79	64.64	1.25
GMP	7.43	1.84	5.51	2.85	1.01	18.26	22.72	38.57	30.22	**0.74**
HM	6.56	2.49	5.72	3.32	0.82	24.05	27.78	45.05	42.91	**0.87**
IDR	0.13	0.001	0.003	0.003	0.002	24.33	42.13	35.33	28.93	3.00
YI	1.07	0.11	0.18	0.13	0.02	30.99	33.69	54.09	58.74	1.64
MP	8.49	1.53	5.83	3.01	1.49	14.57	20.44	32.56	21.39	3.81
STI	0.45	0.07	0.18	0.08	0.01	58.79	62.85	43.29	113.29	2.57
MST_1	0.72	2.15	4.31	2.61	0.46	203.65	224.38	49.08	346.36	2.00
MST_2	0.80	2.56	35.03	2.72	0.16	200.00	206.16	12.73	399.71	13.68
YSI	0.43	0.02	0.02	0.03	0.01	32.89	40.28	63.12	55.33	**1.00**

In bold: High stability ($\sigma^2g \times e/\sigma^2g \leq 1.0$).

σ^2g: Genotypic variance; σ^2ge: Genotype × environment variance; σ^2p: Phenotypic variance; σ^2e: Error variance; GCV: Genotypic coefficient of variation; PCV: Phenotypic coefficient of variation; h^2B: broad sense heritability; GAM: Genetic advance as percent of the mean. Yp: Yield under non-stress conditions; Ys: Yield under stress conditions; ReY: Percent reduction in yield; IDR: Intensity of drought resistance; GMP: Geometric mean productivity; HM: Harmonic mean; MP: Mean productivity; STI: Stress tolerance index; YI: Yield index; YSI: yield stability index; DRI: Drought resistance index; MST_1: Modified stress tolerance index for the non-stress condition; MST_2: Modified stress tolerance index for stress condition.

Table 7. Principal Component Analysis (PCA) of seed yield and drought tolerance indices of ten accessions of cowpea evaluated under differential drought stress in 2019, 2021, and combined seasons

Parameters	2019		2021		Combined		
	PC1	PC2	PC1	PC2	PC1	PC2	PC3
Yp (g)	0.09	**0.98**	**0.93**	-0.34	0.28	**0.72**	**0.62**
Ys (g)	**0.99**	-0.11	**0.95**	0.29	**0.94**	-0.29	-0.07
ReY (%)	**-0.88**	0.48	0.21	**-0.98**	**-0.77**	**0.64**	0.04
DRI	**0.86**	**-0.51**	-0.2	**0.98**	**0.92**	-0.34	-0.07
GMP	**0.94**	0.32	**0.99**	-0.05	**0.96**	0.11	0.19
HM	**0.99**	0.06	**0.99**	0.09	**0.98**	-0.09	0.02
IDR	**0.67**	**0.71**	**0.98**	-0.18	**0.67**	**-0.66**	0.19
YI	**0.94**	0.33	**0.99**	-0.01	**0.98**	0.12	-0.09
MP	**0.99**	-0.11	**0.95**	0.29	**0.77**	0.44	0.46
STI	**0.87**	-0.48	-0.21	**0.98**	**0.76**	**0.63**	-0.15
MST_1	**0.92**	-0.33	**0.55**	**0.83**	**0.57**	**0.73**	-0.37
MST_2	**0.57**	**0.78**	**0.98**	-0.0003	**0.61**	**0.67**	-0.39
YSI	**0.97**	0.09	**0.97**	0.06	**0.77**	**-0.63**	-0.09
Eigenvalue	9.61	3.15	8.94	3.89	8.17	3.57	1.01
Percentage variance	73.90	24.22	68.74	29.96	62.87	27.43	7.73
Cumulative variance (%)	73.90	98.12	68.74	98.70	62.87	90.30	98.03

Bold indicates high loading (≥0.50). PC: Principal Component.

Yp: Yield under non-stress conditions; Ys: Yield under stress conditions; ReY: Percent reduction in yield; IDR: Intensity of drought resistance; GMP: Geometric mean productivity; HM: Harmonic mean; MP: Mean productivity; STI: Stress tolerance index; YI: Yield index; YSI: yield stability index; DRI: Drought resistance index; MST_1: Modified stress tolerance index for the non-stress condition; MST_2: Modified stress tolerance index for stress condition.

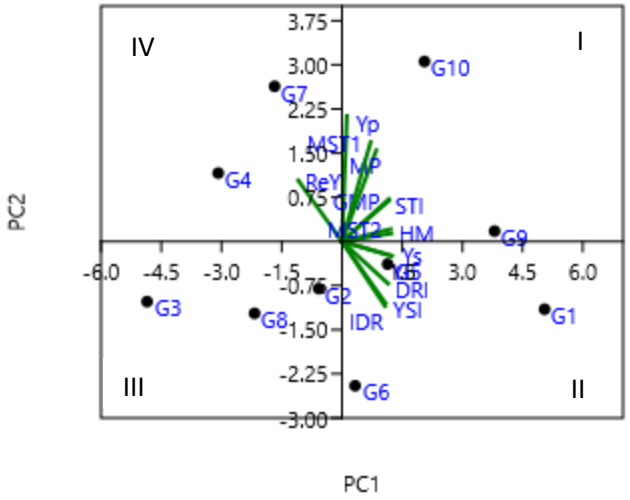

Figure 2. Bi-plot showing the interrelationships among seed yield and drought tolerance indices of ten accessions of cowpeas evaluated under differential drought stress in 2019. Yp: Yield under non-stress conditions; Ys: Yield under stress conditions; ReY: Percent reduction in yield; IDR: Intensity of drought resistance; GMP: Geometric mean productivity; HM: Harmonic mean; MP: Mean productivity; STI: Stress tolerance index; YI: Yield index; YSI: yield stability index; DRI: Drought resistance index; MST_1: Modified stress tolerance index for the non-stress conditions; MST_2: Modified stress tolerance index for stress conditions. G1 – G10 are codes for accessions of cowpea evaluated.

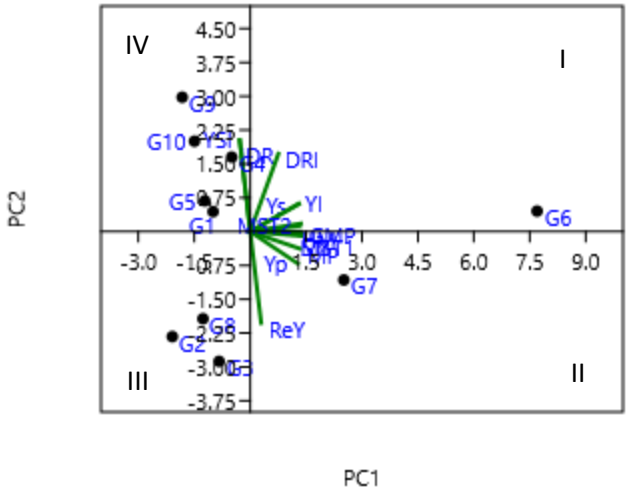

Figure 3. Bi-plot showing the interrelationships among seed yield and drought tolerance indices of ten accessions of cowpeas evaluated under differential drought stress in 2021. Yp: Yield under non-stress conditions; Ys: Yield under stress conditions; ReY: Percent reduction in yield; IDR: Intensity of drought resistance; GMP: Geometric mean productivity; HM: Harmonic mean; MP: Mean productivity; STI: Stress tolerance index; YI: Yield index; YSI: yield stability index; DRI: Drought resistance index; MST_1: Modified stress tolerance index for the non-stress conditions; MST_2: Modified stress tolerance index for stress conditions. G1 – G10 are codes for accessions of cowpea evaluated.

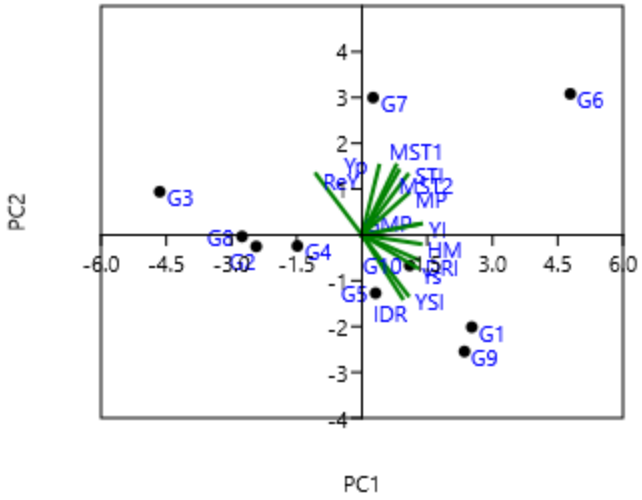

Figure 4. Bi-plot showing the interrelationships among seed yield and drought tolerance indices of ten accessions of cowpeas evaluated under differential drought stress for the combined seasons. Yp: Yield under non-stress conditions; Ys: Yield under stress conditions; ReY: Percent reduction in yield; IDR: Intensity of drought resistance; GMP: Geometric mean productivity; HM: Harmonic mean; MP: Mean productivity; STI: Stress tolerance index; YI: Yield index; YSI: yield stability index; DRI: Drought resistance index; MST_1: Modified stress tolerance index for the non-stress condition; MST_2: Modified stress tolerance index for stress conditions. G1 – G10 are codes for accessions of cowpea evaluated.

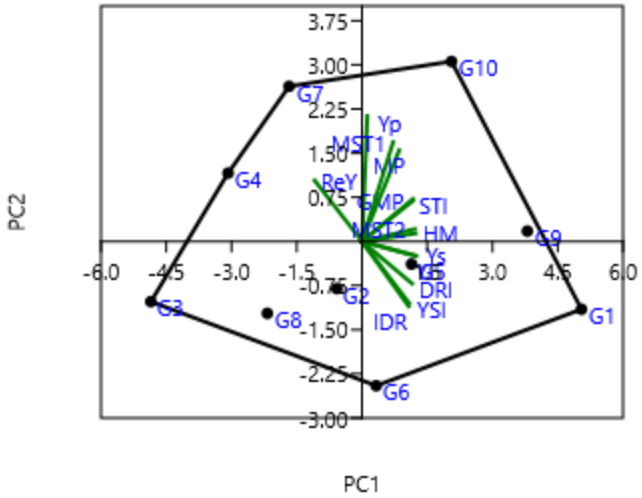

Figure 5. Polygon view of the interrelationships among seed yield and drought tolerance indices of ten accessions of cowpeas evaluated under differential drought stress in 2019. Yp: Yield under non-stress conditions; Ys: Yield under stress conditions; ReY: Percent reduction in yield; IDR: Intensity of drought resistance; GMP: Geometric mean productivity; HM: Harmonic mean; MP: Mean productivity; STI: Stress tolerance index; YI: Yield index; YSI: yield stability index; DRI: Drought resistance index; MST_1: Modified stress tolerance index for the non-stress condition; MST_2: Modified stress tolerance index for stress conditions. G1 – G10 are codes for accessions of cowpea evaluated.

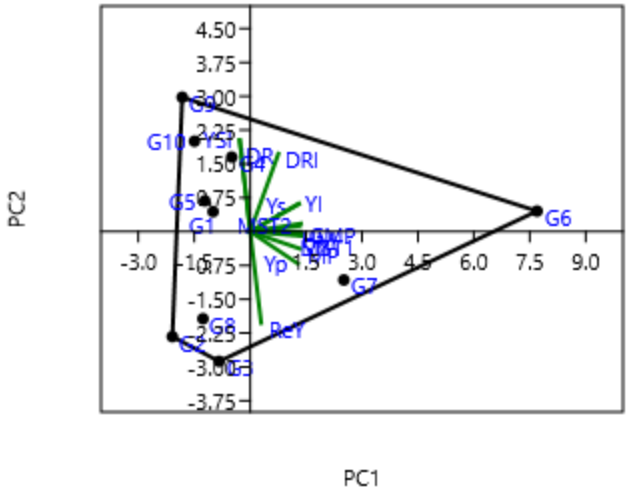

Figure 6. Polygon view of the interrelationships among seed yield and drought tolerance indices of ten accessions of cowpeas evaluated under differential drought stress in 2021. Yp: Yield under non-stress conditions; Ys: Yield under stress conditions; ReY: Percent reduction in yield; IDR: Intensity of drought resistance; GMP: Geometric mean productivity; HM: Harmonic mean; MP: Mean productivity; STI: Stress tolerance index; YI: Yield index; YSI: yield stability index; DRI: Drought resistance index; MST_1: Modified stress tolerance index for the non-stress conditions; MST_2: Modified stress tolerance index for stress conditions. G1 – G10 are codes for accessions of cowpea evaluated.

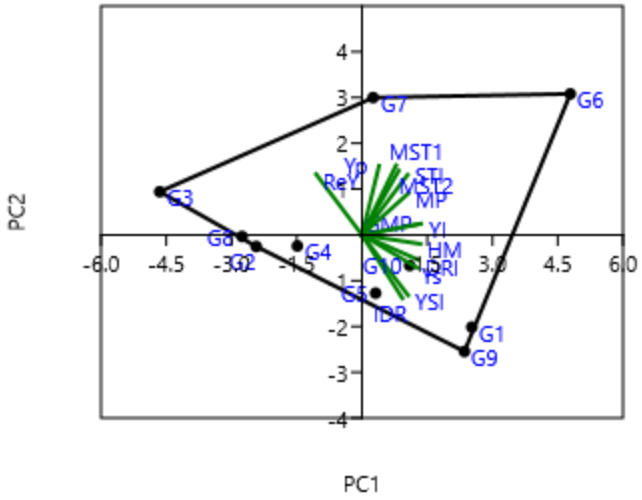

Figure 7. Polygon view of the interrelationships among seed yield and drought tolerance indices of ten accessions of cowpeas evaluated under differential drought stress for the combined seasons. Yp: Yield under non-stress conditions; Ys: Yield under stress conditions; ReY: Percent reduction in yield; IDR: Intensity of drought resistance; GMP: Geometric mean productivity; HM: Harmonic mean; MP: Mean productivity; STI: Stress tolerance index; YI: Yield index; YSI: yield stability index; DRI: Drought resistance index; MST_1: Modified stress tolerance index for the non-stress conditions; MST_2: Modified stress tolerance index for stress conditions. G1 – G10 are codes for accessions of cowpea evaluated.

Table 8. Genotypic correlation among seed yield and drought tolerance indices of cowpea evaluated under differential drought stress in 2019 and 2021

Trait	Year	Yp	Ys	ReY	DRI	GMP	HM	IDR	YI	MP	STI	MST_1	MST_2	YSI
Yp	**2019**	1	-0.04	0.37	-0.22	0.36	0.11	-0.37	-0.05	0.76**	0.34	0.65*	0.12	-0.37
	2021	1	0.82**	0.53	0.31	0.96**	0.91**	-0.53	0.82**	0.99**	0.94**	0.91**	0.87**	-0.53
Ys	**2019**			0.37	0.97**	0.91**	0.98**	0.94**	1.00**	0.61	0.92**	0.71*	0.97**	0.94**
	2021			-0.05	0.79**	0.95**	0.98**	0.05	1.00**	0.89**	0.95**	0.93**	0.05	-1.00**
ReY	**2019**				-0.96**	-0.72*	-0.87**	-1.00**	-0.94**	-0.31	-0.72*	-0.41	-0.83	-1.00**
	2021				-0.64*	0.27	0.14	-1.00**	-0.05	0.39	0.24	0.22	0.18	-1.00**
DRI	**2019**					0.79**	0.91**	0.97**	0.96**	0.45	0.81**	0.54	0.93**	0.97**
	2021					0.57	0.67*	0.65*	0.79**	0.45	0.59	0.61	0.62	0.64*
GMP	**2019**						0.97**	0.72*	0.91**	0.87**	0.99**	0.93**	0.94**	0.72*
	2021						0.99**	-0.27	0.95**	0.99**	0.99**	0.97**	0.95**	-0.14
HM	**2019**							0.87**	0.98**	0.71*	0.96**	0.81**	0.97**	0.88**
	2021							-0.14	0.98**	0.96**	0.99**	0.98**	0.96**	-0.14
IDR	**2019**								0.94**	0.31	0.72*	0.42	0.84**	1.00**
	2021								0.05	-0.39	-0.24	-0.22	-0.17	1.00**
YI	**2019**									0.61	0.92**	0.71*	0.97**	0.94**
	2021									0.89**	0.95**	0.95**	0.93**	0.05
MP	**2019**										0.86**	0.97**	0.72*	0.31
	2021										0.98**	0.95**	0.92**	-0.39
STI	**2019**											0.93**	0.96**	0.72*
	2021											0.99**	0.97**	-0.24
MST_1	**2019**												0.80**	0.41
	2021												1.00**	-0.22
MST_2	**2019**													0.83**
	2021													-0.17

*****: Significant at P ≤ 0.01; *: Significant at P ≤ 0.05.***

Yp: Yield under non-stress conditions; Ys: Yield under stress conditions; ReY: Percent reduction in yield; IDR: Intensity of drought resistance; GMP: Geometric mean productivity; HM: Harmonic mean; MP: Mean productivity; STI: Stress tolerance index; YI: Yield index; YSI: yield stability index; DRI: Drought resistance index; MST_1: Modified stress tolerance index for the non-stress condition; MST_2: Modified stress tolerance index for stress condition.

4. Discussion

Plant breeding programs for drought tolerance principally focus on yield which reflects the adaptability and stability of genotypes. Various drought tolerance indices have been used as key contributors in the selection of drought-tolerant genotypes of crop species. However, their genetic variability and the effect of genotype by environment interaction (GEI) on these indices have not been seriously explored. Variability has three primary components: genotypic (G), environmental (E), and G × E interaction (I). GEI brings ambiguity into the selection process, influencing trait heritability estimates and responsiveness to selection. The variance component ratio of $\sigma^2g\times e/\sigma^2g$ can be used to quantify the magnitude of the GEI to genetic effects. A ratio smaller than 1.0 shows that genetic factors have a larger effect and stability in comparison to the variability associated with the interaction of genotype and environment (Hossain et al., 2013).

The significant mean squares shown regarding seed yield under the differential drought stress indicated high genetic differences among the accessions under both non-stress and drought-stress conditions. The significant genotype × environment and environmental effects for yield and drought tolerance indices indicated that accessions performed differently under differential moisture conditions within each year (environment), and that differences in the environment were significant enough to reveal the differences among genotypes. Similar levels of variations have been reported in such crops as maize (Lao et al., 2022; Badu-apraku et al., 2021), cowpea (Ajayi, 2020; Batieno et al., 2016), peanut (Songsri et al., 2008), sorghum (Choudhary et al., 2021), rice (Hussain et al., 2021), and wheat (Bennani et al., 2017; Al-rawi, 2016). These results also suggested large differences in environmental factors such as soil nutrient status and water holding capacity, ranges of temperatures, and relative humidity of the screen house at the experimental site (Badu-apraku et al., 2021). These findings highlight the importance of considering genetic variation and GEI when studying drought tolerance in cowpeas. The results indicate the need for further investigation into specific cowpea genotypes that exhibit higher seed yield under drought stress conditions, which could contribute to the development of drought-tolerant varieties in cowpea breeding programs. Seed yield in non-stress conditions for the two years was generally higher than that of the drought stress conditions, and the reduction in seed yield was also higher in the first year compared to the value observed in the second year. Overall, an above-average reduction in seed yield was associated with accessions G8, G7, G4, G3, and G2. Mostly, accessions with exceptional performance in non-stress conditions had the highest reduction in seed yield while those with low yield under non-stress did not have their yield seriously affected by drought stress in agreement with Batieno et al. (2016) in cowpea. Above all, the percentage reduction in seed yield stayed within the previously reported range in cowpea (Batieno et al., 2016), wheat (Bennani et al., 2017; Al-rawi, 2016; Guendouz et al., 2021), rice (Hussain et al., 2021), and maize (Bonea, 2020). Even though accessions G3, G7, and G8 were consistent across years with an above-average reduction in yield, no accession had the highest yield in both conditions consistently across years suggesting that indirect selection for drought stress could not be projected based on their performance under optimum conditions (Bennani et al., 2017; Al-rawi, 2016), however, accessions

G6 and G10 had an above-average yield in both conditions for the combined seasons. On average, accessions G1, G9, G10, G6, and G7 which had close to average and above-average yield under non-stress and drought-stress conditions were more drought-resistant and desirable. These accessions are promising accessions for optimum and drought stress conditions as reported for cowpeas (Ajayi, 2020).

Highly significant differences in drought tolerance indices indicated that these indices exhibited high genetic diversity and could discriminate among the accessions under the differential drought stress (Bonea, 2020). The range of each tolerance index obtained in the present study is similar in many cases to the ones previously reported (Anwar et al., 2011; Al-rawi, 2016; Eid and Sabry, 2019; Ajayi, 2020; El haddad et al., 2020; Lao et al., 2022; Sareen et al., 2023; Yahaya et al., 2023). GMP, HM, and ReY exhibited high stability and should be considered in any plant breeding program for drought tolerance. Therefore, accessions such as G1 and G5 exhibiting higher and consistent GMP and HM across environments with a lesser reduction in yield would be more stable. STI combined accessions which hard large differences in seed yield between non-stress and drought stress conditions. GMP, MP, and YI pinpointed accessions desirable under drought-stress conditions in the agreement with (Mahdi, 2012), Al-rawi (2016), and El haddad et al. (2020). Accessions G1 and G6 were the most tolerant accessions according to ranking and combined high values of drought tolerance indices across years; moderately tolerant accessions combined mostly moderate values of the indices across years, while the most susceptible accessions (G8, G2, and G3) combined low values of the indices across years in agreement with the findings of Ajayi (2020), Bonea (2020), Eid and Sabry (2019), Guendouz et al. (2021), Yahaya et al. (2023). Similar trends were also shown by the cluster analysis in agreement with Teklay et al. (2020) and Hussain et al. (2021) who reported the effectiveness of cluster analysis in the classification of genotypes into different classes of drought tolerance. The combined ANOVA results reveal significant genetic variation among cowpea accessions for seed yield and various drought tolerance indices. The effects of the year and the interaction between accession and year highlight the importance of considering environmental factors and GEI in studying drought tolerance in cowpeas. These findings provide valuable insights for further research on identifying and selecting cowpea genotypes with improved drought tolerance.

Based on the rankings provided in the results, where 1 to 5 indicates a high ranking and above-average seed yield is considered high, we can assess whether genotypes with high drought tolerance also exhibited high seed yield under non-stress conditions. In the 2019 season, genotype G1 had a high ranking in several drought tolerance indices (1st or close to the top) and also had a relatively high ranking for seed yield under non-stress conditions (6th). This suggests that G1 exhibited both high drought tolerance and a relatively high seed yield in the absence of drought stress. Other genotypes such as G4, G9, and G10 also had above-average seed yield rankings (2nd, 4th, and 3rd, respectively) and showed varying levels of drought tolerance, although not as consistently high as G1. However, in the 2021 season, genotype G6 had high rankings in most drought tolerance indices (1st or close to the top) and achieved the highest ranking for seed yield

under non-stress conditions. This indicates that G6 exhibited both high drought tolerance and a high seed yield in the absence of drought stress. Other genotypes such as G2, G4, G5, G7, and G8 also had above-average seed yield rankings (6th, 3rd, 4th, 7th, and 8th, respectively) and showed varying levels of drought tolerance. Based on these observations, there is some indication that genotypes with high drought tolerance, as measured by their rankings in drought tolerance indices, also exhibited above-average seed yield under non-stress conditions.

A combination of high GCV and PCV for such parameters as seed yield under drought stress, ReY, DRI, HM, IDR, YI, STI, MST_1, MST_2, and YSI indicated that the accessions had a broad genetic base for these parameters, suggesting that selection for them would be effective. Moderate GCV showed by parameters such as seed yield in non-stress conditions, GMP, and MP indicated the existence of moderate variability among the studied accessions for these parameters. Furthermore, higher PCV compared to GCV indicated the influence of the environment on these parameters. However, the influence of the environment was minimal on most of the parameters which suggests that they are amenable to improvement. These results agree with the findings of Anwar et al. (2011) and Eid and Sabry (2019). High broad sense heritability coupled with high GAM exhibited among parameters such as DRI, YSI, and ReY indicate that they are governed by additive gene effects and hence selection for them would be effective. These results agree with Bennani et al. (2017) on ReY; Anwar et al. (2011), and Ajayi (2020) on YSI and DRI. Apart from MST_2 which showed low heritability, other parameters had moderate to high heritability combined with high GAM, indicating that the parameters were less influenced by the effect of the environment, making them effectively transmitted to the progeny. Seed yield also exhibited lower heritability under drought stress compared to the non-stress condition as reported by Bogale et al. (2012), Sellammal et al. (2014), and Ajayi (2020), in maize, rice, and cowpea, respectively. Information on the heritability of drought-tolerant traits is important in that it determines the degree to which improvement based on selection is possible (El-Rawy and Hassan, 2014). Hence, moderate to high heritability combined with high GAM exhibited among accessions for the yield and most of the drought tolerance indices indicated that these parameters can be directly used as selection criteria for yield enhancement of cowpeas for drought stress. Overall, the combination of moderate to high heritability and high GAM provides strong support for the effectiveness of breeding efforts in improving drought tolerance in cowpeas. It indicates that genetic improvement through selection is feasible and can lead to the development of drought-tolerant varieties with enhanced performance and productivity under water-limited conditions. This information can be practically utilized in selecting superior genotypes of cowpeas in ways such as phenotypic evaluation, determination of selection criteria, genetic gain estimation, multi-trait selection, selection indices, replication, and validation.

The extracted PCs (1 and 2) accounted for the highest variability of more than 90 percent of the total variation indicating a successful PCA according to Hammer et al. (2001). Therefore, selection based on the first two PCs is appropriate. All parameters were important contributors to PC1 consistently in both years and combined seasons except seed yield in the non-stress condition in

2019 and combined years respectively, and ReY, DRI, and STI in 2021. However, yield in non-stress conditions was among the major contributors in PC2 of 2019 and combined years. Overall, PC1 can be referred to as drought tolerant and yield potential component (accessions with high tolerance and high yield in both conditions were highly associated with this axis), while PC2 can be regarded as a yield potential component (high yielding accessions under optimum conditions are strongly associated with this axis). The present findings are similar to Batieno et al. (2016), Ajayi (2020), and Sanogo et al. (2023) in cowpea, Teklay et al. (2020), and Choudhary et al. (2021) in sorghum, Guendouz et al. (2021) in wheat, Lao et al. (2022) in maize, and Padmashree et al. (2023) in rice. For the biplot analyses, different trends of relationships were observed under different years because of the G × E interaction effects. The combined biplot may be regarded as the representative of the results across years; a high positive correlation between yield in non-stress conditions with MST_1, MST_2, STI, MP, GMP, and YI indicated that these indices are capable of selecting accessions for optimum conditions. However, the positive correlation of yield under drought stress with indices such as GMP, YI, HM, DRI, YSI, and IDR indicated that these indices were more effective at selecting accessions with superior performance under drought stress conditions. Nevertheless, a high, positive correlation of GMP and YI with seed yield under drought stress and non-stress conditions indicated that selection for these indices will pinpoint superior accessions in both drought stress and non-stress conditions. Therefore, the combination of these indices selected both the highly tolerant accessions such as G6, G1, G9, and G10 and the moderately tolerant G7 and G5. The polygon view of the biplot identified the best accessions for a specific trait or a group of traits in the study. Accessions G6, G7, G9, G2, and G3 vertex accessions, hence, were the most responsive for the combined seasons. Vertex accessions exhibit higher values for the traits contained within the same sector in the biplot (Atnaf et al., 2017). Therefore, G7 had the highest seed yield under non-stress conditions, G6 had higher values for drought tolerance indices such as MST_1, MST_2; G9 combined higher values of YSI, IDR, and DRI with seed yield under drought stress conditions, G3 had the highest values for a reduction in yield while G2 had no corresponding trait nor indices in its sector.

Genotypic correlation analysis was done among parameters to determine the most suitable tolerance indices. Previous reports have indicated that the most suitable indices for the selection of drought-tolerant genotypes are those that show a positive correlation with grain yield in both the conditions of drought stress and non-stress (Al-rawi, 2016; Bonea, 2020; Hosseini et al., 2020). The lack of correlation between yield in non-stress and drought stress conditions in 2019 suggests that higher yield under non-stress conditions does not always anticipate high yield under drought stress conditions (Ajayi, 2020). This agrees with Bonea (2020) in maize. On the contrary, the high positive correlation of seed yield in non-stress conditions with seed yield under drought stress, GMP, HM, YI, MP, STI, MST_1, and MST_2 in 2021 indicated that these indices can discriminate accessions exhibiting superior performance under both drought and non-stress conditions from the others and would be the best indices to screen accessions of cowpea under drought stress. These results align with the findings of Hussain et al. (2021) for GMP and STI, El haddad et al. (2020) for STI, GMP, MP, and HM, and also the findings of Teklay et al. (2020) for MP, HM, GMP, STI,

and YI. The importance of MP, MST_1, STI, GMP, and HM for selection under both stress and non-stress conditions has been emphasized by Bennani et al. (2017) in agreement with the present study. Lao et al. (2022) stated that GMP, MP, and STI should be the preferred indices for screening drought-tolerant maize genotypes. A consistently significant positive correlation of MST_1 and MP with seed yield under non-stress indicates that these indices are useful in discriminating superior accessions under optimum conditions, which corroborates the biplot results. However, the consistently high positive correlation of seed yield under stress with DRI, GMP, HM, YI, STI, MST_1, and YSI indicated that these indices are effective at discriminating superior accessions under drought stress conditions in agreement with El-Rawy and Hassan (2014) for HM, STI, and YSI, and Ajayi (2020) for DRI, GMP, YI, and YSI. The newly introduced IDR exhibited a high positive correlation with the seed yield under drought stress in 2019 and was only useful for selection under drought stress. Furthermore, the following interaction was consistent across the two years: higher DRI was associated with higher HM, IDR, YI, and YSI. Higher GMP was associated with higher HM, YI, MP, STI, MST_1, and MST_2. Higher MP was associated with higher STI, MST_1, and MST_2. Higher YI was associated with higher STI, MST_1, and MST_2. Higher IDR was associated with higher YSI. Higher HM was associated with higher YI, MP, STI, MST_1, and MST_2. Higher STI was associated with higher MST_1 and MST_2. Higher MST_1 was associated with higher MST_2. However, a higher percent reduction (ReY) was consistently negatively associated with higher DRI, IDR, and YSI which indicated selection based on these indices would discriminate accessions exhibiting a higher level of resistance to yield loss under drought stress. Higher positive correlations indicate similar capabilities of discriminating accessions under drought stress.

5. Conclusion

This study, which reveals that drought significantly reduces seed yield in cowpeas, shows that seed yield and all drought tolerance indices are greatly influenced by genotype effect, environment (year), and genotype x environment interaction. However, the magnitude of G × E about genetic effects indicated high stability of GMP, HM, and ReY. All analyses pinpointed highly tolerant accessions (G1 and G6) from the highly susceptible ones (G2, G3, and G8). Genotypes with high drought tolerance generally exhibited better seed yield under drought stress conditions, indicating their suitability for cultivation in arid and semi-arid regions. However, the study also identified genotypes that displayed high seed yield in the absence of drought stress, suggesting the presence of genotypes with both high drought tolerance and high seed yield potential in non-stress conditions. This study also confirmed MST_1, MST_2, STI, and MP as suitable for selecting high-yielding accessions for non-stress conditions and hence are recommended for optimum conditions. HM, DRI, YSI, and IDR were the most suitable for selecting drought-tolerant accessions and hence recommended for environments prone to drought while GMP and YI were effective under both non-stress and drought-stress conditions. Furthermore, all the indices showed moderate to high heritability and high GAM except MST_2 which showed low heritability. The results of the correlation analysis highlighted the relationships between various drought tolerance traits and seed

yield. Positive correlations were observed between seed yield under non-stress conditions and traits such as yield under stress conditions, DRI, GMP, and MP. Similarly, Yield under stress showed positive correlations with ReY, DRI, GMP, and other productivity indices, indicating their relevance for drought tolerance and productivity improvement. Nonetheless, it is recommended that in-depth multi-environment studies using Additive Main Effects and Multiplicative Interaction (AMMI), Genotype and Genotype × Environment (GGE), and Finlay and Wilkinson (FW) analyses should be conducted to shed more light on the importance of GEI on drought tolerance indices of cowpea for its improvement.

Acknowledgment

The International Institute of Tropical Agriculture (IITA), Ibadan, Nigeria is acknowledged for providing the cowpea accessions used for this study. The Department of Plant Science and Biotechnology, Adekunle Ajasin University, Akungba-Akoko, Nigeria is also acknowledged for providing the screen house and other facilities for the study.

References

Adetumbi, J.A., Akinyosoye, S.T., Agbeleye, A., Kareem, K.T., Oduwaye, O.F., Adebayo, G.G., Olakojo, S.A. 2019. Genetic variability in the agronomic traits, inheritance pattern of seed coat colour, and response to brown blotch disease among cowpea hybrids, Euphytica, 215: 142.

Ajayi, A.T., Adekola, M.O., Taiwo, B.H., Azuh, V.O. 2014. Character expression and differences in yield potential of ten genotypes of cowpea (*Vigna unguiculata* L. Walp), International Journal of Plant Research, 4(3): 63–71.

Ajayi, A.T., Gbadamosi, A.E., Olumekun, V.O., Nwosu, P.O. 2020. GT biplot analysis of shoot traits indicating drought tolerance in cowpea [*Vigna unguiculata* (L.) Walp] accessions at vegetative stage, International Journal of BioSciences and Technology, 13(2): 18–33.

Ajayi, A.T., Gbadamosi, A.E., Osekita, O.S., Taiwo, B.H., Fawibe, A.B., Adedeji, I., Omisakin, T. 2022. Genotype × environment interaction and adaptation of cowpea genotypes across six planting seasons, Frontiers in Life Sciences and Related Technologies, 3(1): 7–15.

Ajayi, A.T. 2020. Relationships among drought tolerance indices and yield characters of cowpea (*Vigna unguiculata* L. Walp), International Journal of Scientific Research in Biological Sciences, 7(5): 93–103.

Al-rawi, I.M.D. 2016. Study of drought tolerance indices in some bread and durum wheat cultivars, Jordan Journal of Agricultural Sciences, 12(4): 1125–1139.

Anwar, J., Subhani, G.M., Hussain, M., Ahmad, J., Hussain, M., Munir, M. 2011. Drought tolerance indices and their correlation with yield in exotic wheat genotypes, Pakistan Journal of Botany, 43(3): 1527–1530.

Atnaf, M., Tesfaye, K., Wegary, D. 2017. Genotype by trait biplot analysis to study associations

and profiles of Ethiopian white lupin (*Lupinus albus* L.) landraces, Australian Journal of Crop Science, 11(1): 55–62.

Badu-apraku, B., Obesesan, O., Abiodun, A., Obeng-Bio, E. 2021. Genetic gains from selection for drought tolerance during three breeding periods in extra-early maturing maize hybrids under drought and rainfed environments, Agronomy, 11: 831.

Batieno, B.J., Tignegreb, J., Hamadouc, S., Hamadoud, Z., Ouedraogoe, T.J., Danquahf, E. Oforig, K. 2016. Field assessment of cowpea genotypes for drought tolerance, International Journal of Sciences: Basic and Applied Research, 30(4): 358–369.

Bennani, S., Nsarellah, N., Jlibene, M., Tadesse, W., Birouk, A., Ouabbou, H. 2017. Efficiency of drought tolerance indices under different stress severities for bread wheat selection, Australian Journal of Crop Science, 11(4): 395–405.

Bogale, G., Rensburg, J.B.J., van Deventer, C.S. 2012. Heritability of drought adaptive traits and relationships with grain yield in maize grown under a high plant population, Ethiopian Journal of Agricultural Sciences, 22(1): 126–126.

Bonea, D. 2020. Grain yield and drought tolerance indices in maize hybrids, Notulae Scientia Biologicae, 12(2): 376–386.

Bouslama, M., Schapaugh, W.T. 1984. Stress tolerance in soybean. I. Evaluation of three screening techniques for heat and drought tolerance, Crop Science, 24: 933–937.

Choudhary, R.S., Biradar, D.P., Katageri, I.S. 2021. Evaluation of sorghum RILs for moisture stress tolerance using drought tolerance indices, The Pharma Innovation Journal, 10(4): 39–45.

de Nóvoa Pinto, J.V., Sousa, D., de P. Nunes, H.G.G.C., de Souza, E.B., de Melo-Abreu, J.P., Sousa, A.M.L., de Souza, P.J.O.P. 2021. Impacts of climate changes on risk zoning for cowpea in the Amazonian tropical conditions, Bragantia, 80: e5521.

Eid, M.H., Sabry, S. 2019. Assessment of variability for drought tolerance indices in some wheat (*Triticum aestivum* L.) genotypes, Egyptian Journal of Agronomy, 41(2): 79–91.

El haddad, N., Rajendran, K., Smouni, A., Es-Safi, N.E., Benbrahim, N., Mentag, R., Nayyar, H., Maalouf, F., Kumar, S. 2020. Screening the FIGS set of lentil (*Lens culinaris* Medikus) germplasm for tolerance to terminal heat and combined drought-heat stress, Agronomy, 10: 1036.

El-Rawy, M.A., Hassan, M.I. 2014. Effectiveness of drought tolerance indices to identify tolerant genotypes in bread wheat (*Triticum aestivum* L.), Journal of Crop Science and Biotechnology, 17(4): 255–266.

FAOSTAT. 2022. Official Website of Food and Agriculture Organization, FAOSTAT_data_8-29-2020-Excel, http://faostat.fao.org, Last Accessed on January 29, 2022.

Farshadfar, F., Sutka, J. 2002. Screening drought tolerance criteria in maize, Acta Agron Hung,

50(4): 411–416.

Fayeun, L.S., Hammed, L.A., Oduwaye, O.A., Madike, J.U., Ushie, E.U. 2016. Estimates of genetic variability for seedling traits in fluted pumpkin (*Telfairia occidentalis* Hook. F), Plant Breeding and Biotechnology, 4(2): 262–270.

Fernandez, G.C.J. 1992. Effective selection criteria for assessing plant stress tolerance, Proceedings of the Symposium Taiwan, 25: 257–270.

Fisher, R.A., Yates, F. 1963. Statistical tables for biological, agricultural, and medical research, Biometrical Journal, 13(4): 225–286.

Gavuzzi, P., Rizza, F., Palumbo, M., Campaline, R.G., Ricciardi G.L., Borghi, B. 1997. Evaluation of field and laboratory predictors of drought and heat tolerance in winter cereals, Canadian Journal of Plant Science, 77: 523–531.

Guendouz, A., Frih, B., Oulmi, A. 2021. Canopy cover temperature and drought tolerance indices in durum wheat (*Triticum durum* Desf.) genotypes under the semi-arid condition in Algeria, International Journal of Bio-Resource and Stress Management, 12(6): 638–644.

Hammer, Ø., Harper, D.A.T., Ryan, P.D. 2001. PAST: Paleontological statistics software package for data analysis, Palaeontologia Electronica, 4(1): 9.

Hossain, K.G., Islam, N., Jacob, D., Ghavami, F., Tucker, M., Kowalski, T., Leilani, A., Zacharias, J. 2013. Interdependence of genotype and growing site on seed mineral compositions in common bean, Asian Journal of Plant Sciences, 12(1): 11–20.

Hosseini, A.D., Dadkhodaie, A., Heidari, B., Kazemeini, S.A. 2020. Evaluation of a hexaploid wheat collection (*Triticum aestivum* L.) under drought stress conditions using stress tolerance indices, Annual Research and Review in Biology, 34(6): 1–10.

Hussain, T., Hussain, N., Ahmed, M., Nualsri, C., Duangpan, S. 2021. Responses of lowland rice genotypes under terminal water stress and identification of drought tolerance to stabilize rice productivity in southern Thailand, Plants, 10: 2565.

Kristin, A.S., Senra, R.R., Perez, F.I., Enriquez, B.C., Gallegos, J.A.A., Vallego, P.R., Wassimi, N., Kelley, J.D. 1997. Improving common bean performance under drought stress, Crop Science, 37: 43–50.

Lao, Y., Dong, Y., Shi, Y., Wang, Y., Xu, S., Xue, J., Zhang, X. 2022. Evaluation of drought tolerance in maize inbred lines selected from the Shaan A group and Shaan B group, Agriculture, 12: 11.

Mahdi, Z. 2012. Evaluation of drought tolerance indices for the selection of Iranian barley (*Hordeum vulgare*) cultivars, African Journal of Biotechnology, 11(93): 15975–15981.

Moosavi, S.S., Samadi, B.Y., Naghavi, M.R., Zali, A.A., Dashti, H., Pourshahbazi, A. 2008.

Introduction of new indices to identify relative drought tolerance and resistance in wheat cultivars, Desert, 12: 165–178.

Nauditt, A., Stahl, K., Rodríguez, E., Birkel, C., Formiga-Johnsson, R.M., Kallio, M., Ribbe, L., Baez-Villanueva, O.M., Thurner, J., Hann, H. 2022. Evaluating tropical drought risk by combining open access gridded vulnerability and hazard data products, Science of the Total Environment, 882: 153493.

Ogbaga, C.C., Stepien, P., Johnson, G.N. 2014. Sorghum (*Sorghum bicolor*) varieties adopt strongly contrasting strategies in response to drought, Physiologia Plantarum, 152(2): 389–401.

Padmashree, R., Reddy, V., Mogar, N.D., Barbadikar, K.M., Balakrishnan, D., Gireesh, C., Siddaiah, A.M., Badri, J., Lokesha, R., Ramesha, Y.M., Senguttuvel, P., Diwan, J.R., Madhav, M.S., Rani, S.C., Sundaram, R.M. 2023. Assessment of multiple tolerance indices to identify rice lines suitable for aerobic system cultivation, International Journal of Plant and Soil Science, 35(11): 16–28.

Rosielle, A.A., Hamblin, J. 1981. Theoretical aspects of selection for yield in stress and non-stress environments, Crop Science, 21: 943–946.

Sanogo, S.A., Diallo, S., Batieno, T.B., Ishola, A.I., Sawadogo, N., Nyadanu, D. 2023. Screen house assessment of cowpea genotypes for drought tolerance using selection indices, Agricultural Sciences, 14: 457–473.

Sareen, S., Budhlakoti, N., Mishra, K.K., Bharad, S., Potdukhe, N.R., Tyagi, B.S., Singh, G.P. 2023. Resilience to terminal drought, heat, and their combination stress in wheat genotypes, Agronomy, 13: 891.

Sellammal, R., Robin, S., Raveendran, M. 2014. Association and heritability studies for drought resistance under varied moisture stress regimes in backcross inbred population of rice, Rice Science, 21(3): 150–161.

Songsri, P., Jogloy, S., Kesmala, T., Vorasoot, N., Akkasaeng, C., Patanothai, A., Holbrook, C.C. 2008. Heritability of drought resistance traits and correlation of drought resistance and agronomic traits in peanut, Crop Science, 48(6): 2245–2253.

Teklay, A., Gurja, B., Taye, T., Gemechu, K. 2020. Selection efficiency of yield-based drought tolerance indices to identify superior sorghum [*Sorghum bicolor* (L.) Moench] near-isogenic lines (NILs) under two-contrasting environments, African Journal of Agricultural Research, 15(3): 379–392.

Yahaya, M.A., Shimelis, H., Nebie, B., Mashilo, J., Pop, G. 2023. Response of African sorghum genotypes for drought tolerance under variable environments, Agronomy, 13: 557.